Agricultural Water Management 319 (2025) 109761

Contents lists available at ScienceDirect

Agricultural Water Management

journal homepage: www.elsevier.com/locate/agwat

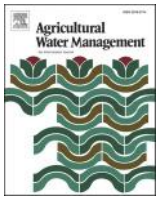

The potential of novel remote sensing evapotranspiration data and global soil maps for SWAT+ agro-hydrological modeling in data-scarce regions of the North Mediterranean

Ismail Bouizrou [a,b,*], Giulio Castelli [b,c,d], Gonzalo Anibal Cabrera [b], Lorenzo Villani [b], Stavros Solomos [e], Giorgos Maneas [f], Christos Pantazis [e,f], Elena Bresci [b]

[a] Institute for Ecology and Landscape, Hochschule Weihenstephan-Triesdorf University of applied Sciences, Germany
[b] Department of Agriculture, Food, Environment and Forestry (DAGRI), University of Florence, Italy
[c] Environmental Governance and Territorial Development Hub (GEDT), University of Geneva, Switzerland
[d] UNESCO Chair in Hydropolitics, University of Geneva, Switzerland
[e] Research Centre of Atmospheric Physics and Climatology, Academy of Athens, Greece
[f] Navarino Environmental Observatory (N.E.O.), Messenia, Greece

ARTICLE INFO

Keywords:
Olive farming
Agricultural management practice
Soil degradation
Water resource management
Modeling tool
Multisite calibration

ABSTRACT

Mediterranean ecosystems are increasingly affected by rising temperatures, shifting precipitation patterns and water resource overexploitation, while limited ground-based data challenge effective land and water management. The Messinia region in the southwestern Greece is severely affected by soil degradation and inadequate water management practices. Covering about 70 % of olive farming, the region plays a crucial role in the regional agricultural economy. The study uses the SWAT+ model for comprehensive agro-hydrological modeling and multisite calibration of four ungauged watersheds in the Messinia region. It integrates remotely sensed evapotranspiration data as reference data, high-resolution global soil maps and agricultural practices (planting, irrigation, and harvesting). The results show that incorporating DSOLMap soil data improved simulations over a local soil map. Additionally, GLEAM, aligns better with FAO-56 method and offers a more accurate representation of AET than MODIS in the Messinia region. Our findings are in line with the literature which reports that GLEAM accounts for soil moisture and vegetation dynamics while MODIS has known limitations in capturing irrigation effects and fine-scale variability. The SWAT+ model using GLEAM, DSOLMap, and management schedules achieved the best results (NSE > 0.5; PBIAS $< \pm 15$ %), outperforming other model setups, particularly when compared to MODIS-based simulations which showed underperformance. This approach that combines SWAT+ with remote sensing and integrates management schedules, offers a more accurate representation of the water cycle and enhances water resource management in data-scarce regions. Additionally, the approach is scalable and replicable in other data-scarce regions and offers a valuable tool for site-specific management strategies.

1. Introduction

The Mediterranean region is currently experiencing the impacts of climate change, such as rising temperatures and shifting precipitation patterns, in addition to the overexploitation of water resources (IPCC, 2021; MedECC, 2020). This region is increasingly becoming arid with reduced precipitation and increased evapotranspiration, which are modifying hydrological processes (IPCC, 2021; Tramblay et al., 2020). This combined effect has a significant impact on agricultural production and water resources, where sustainable water and land management requires a deeper understanding of hydrological processes, including evapotranspiration, soil infiltration and runoff generation (Bronstert and Plate, 1997; Clark et al., 2015).

In this regard, agro-hydrological models are powerful tools to accurately evaluate the water balance and consequently are highly relevant for water resource management at the watershed scale (Lu et al., 2018; Tessema, 2011). Physically-based distributed models that consider spatial variations in hydrological processes are particularly

* Correspondence to: A1.511, Am Hofgarten 1, Freising 85354, Germany.
E-mail address: ismail.bouizrou@hswt.de (I. Bouizrou).

https://doi.org/10.1016/j.agwat.2025.109761
Received 14 April 2025; Received in revised form 12 August 2025; Accepted 17 August 2025
Available online 29 August 2025

important for assessing the impact of management practices on water availability (Kofidou and Gemitzi, 2023; Paniconi and Putti, 2015). The Soil and Water Assessment Tool (SWAT) (Arnold et al., 1998) is widely used for studies related to water resource management and climate change impact assessments particularly in the Mediteranean region (i.e., Aqnouy et al., 2023; Taia et al., 2023; Villani et al., 2024a). similarly, the Water Evaluation and Planning System (Yates et al., 2007) is often used for water resource management and agricultural planning (i.e., Amin et al., 2018; Bañares et al., 2024; Mehboob and Kim, 2021). The Variable Infiltration Capacity Model (VIC) (Liang et al., 1994) is known for simulating land-atmosphere interactions and has been used in several agro-hydrological studies focusing on water balance and crop yield prediction (i.e., Himanshu et al., 2023; Srivastava et al., 2020). Furthermore, the HYDRUS (Simunek et al., 1999) is also frequently applied to model water and solute movement in variably saturated soil profiles for soil-water interactions in agricultural fields (i.e., Dou et al., 2022). Among these models, the SWAT model is the most commonly used agro-hydrological model globally (Fu et al., 2019), as it integrates hydrological dynamics with management practices to simulate processes such as evapotranspiration, crop growth and surface runoff (Akoko et al., 2021; Eini et al., 2023; Villani et al., 2024a). An enhanced version, SWAT+ was recently developed (Bieger et al., 2019; Wagner et al., 2022) and offers a more flexible and improved spatial representation of watershed interactions and processes by allowing multiple land uses, soils and management practices within each subbasin. Furthermore, SWAT+ incorporates management practices, allows for code modifications to adapt to specific needs and enables users to customize individual components and define user-specific functions (Yen et al., 2019). However, the application of these highly parameterized models has always been a challenging task due to their demand for a significant amount of input observations.

One of the most important challenges for modelers working in small Mediterranean watersheds is the scarcity of high-quality, extended ground-based data, as many watersheds are either poorly gauged or ungauged. Earth observation datasets sourced from remote sensing (RS) and high-resolution global products constitute a promising solution (Nourani et al., 2021; Sun et al., 2019) which can be used as an effective alternative to ground-based measurements. Over the past few years, RS products have gained notable success as a result of rapid advances in computing power, satellite technology, data storage and the availability of large datasets (Razavi, 2021). The RS methods can significantly contribute to hydrological modeling by accurately simulating variables such as streamflow (Gleason and Durand, 2020; Jiang and Wang, 2019; Winsemius et al., 2008). Moreover, RS datasets are valuable in hydrology for model inputs such as meteorological data and as reference data for the calibration-validation process, including simulating evapotranspiration (ET) that is a key component of the hydrological cycle.

Accurate estimation of ET is crucial for evaluating water resources and agricultural management (Falamarzia et al., 2014; Kadam et al., 2021; Loukas et al., 2005; Visakh et al., 2019). This is particularly important in semi-arid areas, in which most precipitation is lost through evapotranspiration. Recently, remotely sensed evapotranspiration (RS-ET) data have gained crucial importance for hydrological model calibration by providing spatio-temporally distributed calibration data. Moreover, it serves as a comprehensive indicator of surface water availability (Rajib et al., 2018; Rientjes et al., 2013; Tobin and Bennett, 2017). Advances in numerical tools and RS technology have significantly improved the estimation of evapotranspiration and increased its use for agro-hydrological model evaluation. Consequently, a wide range of actual evapotranspiration (RS AET) datasets are freely available with different levels of complexity. In current RS AET studies, the Global Land Evaporation Amsterdam Model (GLEAM) and the Moderate Resolution Imaging Spectroradiometer (MODIS) are the two most widely used products worldwide (Tobin and Bennett, 2017). GLEAM and MODIS represent two different approaches that have been validated against ground-based eddy covariance tower measurements. They use different algorithms and estimation methods and retrieve AET at different spatial and temporal resolutions. Furthermore, their reliability has been evaluated in recent studies. Qiao et al. (2022) evaluated SWAT AET and MODIS against ET measurements using eddy covariance (EC) data. They found that MODIS and SWAT estimates of ET were more consistent with EC measurements for the tall-grass prairie compared to the mixed-grass prairie, with SWAT showing better performance. Similarly, Koltsida and Kallioras (2022) used monthly streamflow data and MODIS AET to assess the multivariate calibration of a sub-basin with mixed land use in Greece. They demonstrated the usefulness of MODIS when combined with streamflow data to enhance simulation performance, making it a suitable choice for watersheds in data-scarce regions. Furthermore, Odusanya et al. (2019) combined GLEAM AET data and the SWAT model to simulate AET in the Ogun River Basin watershed in Nigeria, showing the potential of GLEAM AET for calibrating and validating SWAT with reasonable accuracy in large data-scarce basins. Roy et al. (2017) demonstrated the accuracy of GLEAM for evapotranspiration estimation and its role in improving streamflow simulation in data-scarce regions of Tanzania and Kenya. Consistent with previous research, the effectiveness of RS-ET for model configuration and calibration varies with model complexity, topography, region, and climatic conditions. Thus, no single product is universally applicable. Accordingly, it was decided to compare the two AET products, MODIS and GLEAM which are characterized by fundamental differences, to evaluate and select the most appropriate product for the Messinia data-scarce region.

Soil is another important factor influencing water balance processes, and therefore plays a crucial role in hydrology (Merz and Mosley, 1998). Spatial variability of soil and its hydraulic properties has been found to directly affect and modify hydrological response at the watershed scale (Centeno et al., 2020; Fatichi et al., 2016; Tenreiro et al., 2020). Accurate data on soil properties are paramount for developing spatially distributed hydrological models, particularly at small spatial scales (Wahren et al., 2016). Yet soil surveys at watershed scale are time-consuming, costly and often limited to a single soil layer, limiting the availability of spatially distributed soil information, particularly in data-scarce regions (Moore et al., 1993; Rivas-Tabares et al., 2020). In this context, global soil databases have become increasingly used as alternative sources of ground-based soil data for hydrological models, due to the progress of remote sensing and machine learning algorithms (Hengl and MacMillan, 2019). The Harmonized World Soil Database (HWSD; (ISRIC, ISS-CAS, FAO; FAO et al., 2012)) and the Digital World Soil Map (DSWM; FAO, 2003a, 2003b) are two global soil databases used extensively for the SWAT model (Abbaspour et al., 2019; Dai et al., 2019). However, both databases have low spatial resolutions, 1 km for HWSD and 5 km for DSWM, which can increase model uncertainty. Recently, a new high-resolution global soil map (DSOLMap, López-Ballesteros et al., 2023) was developed and tailored to SWAT+ format. It offers a high spatial resolution (250 m) with a more detailed soil profile divided into six horizons. It was processed using 3D machine learning based on soil profile observations from over 350000 training points (Hengl and MacMillan, 2019). In addition, DSOLMap was successfully evaluated against DSWM and HWSD using the SWAT+ model on daily and monthly timesteps to simulate streamflow and estimate hydrological processes in the northern part of Spain (López-Ballesteros et al., 2023). The authors indicated that DSOLMap provided a better representation of the daily watershed hydrological response, with only DSOLMap achieving satisfactory performance in streamflow simulation using SWAT+ . Globally, there is a shortage of studies comparing various soil input data for hydrological modeling and evaluating new global soil databases (Huang et al., 2022). In the Mediterranean region, only a limited number of studies have examined the impact of different soil inputs on agro-hydrological modeling. Wahren et al. (2016) combined digital soil mapping with the SWAT model in a data-scarce Mediterranean watershed in north-central Portugal, highlighting the importance of spatially distributed soil information for small watershed modeling and improved river basin management. Similarly,

Rivas-Tabares et al. (2020) compared a low-resolution global soil dataset (HWSD) with two high-resolution datasets derived from the SOM algorithm to assess their impact on key hydrological components using the SWAT model. Their findings demonstrated that the SOM-based approach significantly enhanced the accuracy of streamflow simulations in a semi-arid Mediterranean watershed. While these studies evaluated the effects of different soil input data on streamflow, no study has assessed their impact on other components of the water cycle, particularly evapotranspiration.

The Messinia region is in the Southwestern Peloponnese, Greece. Despite the importance of its natural ecosystems which include the Gialova Lagoon selected as Natura2000 site is a data-sparse area with most watersheds being ungauged and limited information about soil characteristics. The availability of water resources in this typical North Mediterranean region is significantly affected by climate change, including increasing temperatures, decreasing precipitation patterns, and a reduction in annual streamflow as well as inadequate land and water management practices (Klein et al., 2015). In this context, a comprehensive modeling approach that integrates remote sensing and incorporating detailed agricultural management practices is needed for better estimating hydrological processes and providing useful insights for sustainable water and land management. In Messinia, we conducted this research as part of the SALAM-MED project (https://www.salam-med.org/), funded under the PRIMA S1 2021 programme supported by the European Union (Desertification Research Center, University of Sassari, 2021). The project is intended to improve watershed hydrology and soil fertility in the region by combining biological and digital agricultural technologies with modeling approaches. This study aims to highlight the importance of using freely available global and high-resolution RS datasets for water balance simulations at the scale of small watersheds. Few studies have assessed the performance of multiple RS-ET datasets for calibration and validation in hydrological simulations across the North-East Mediterranean region, including Greece, with no prior research conducted in the Messinia region. To the best of our knowledge, no study in the Mediterranean has compared the effects of high-resolution global soil data and local soil maps on hydrological modeling of evapotranspiration. Additionally, studies integrating remote sensing, soil map analysis and agro-hydrological models remain relatively uncommon in this region. Accordingly, the objectives of this paper are to: (1) explore the potential of multiple RS-ET products for SWAT+ model evaluation using a multisite calibration approach; (2) evaluate the performance of a recent high-resolution global soil database in constraining hydrological models compared to data from local soil map; and (3) investigate modifying agricultural land use using crop distribution statistics and integrating management details into SWAT+ to enhance model performance and improve agricultural water management in data-scarce regions.

2. Materials and methods

2.1. Study area

The Messinia region (37°8'31.21" N, 21°57'7.96" E) is located in the southwestern Peloponnese, Greece. It includes four watersheds, namely Sellas, Xerolagados, Gianouzagas, and Xerias (Ekstedt, 2013; Klein et al., 2015), covering a total area of 210 km^2. The headwaters originate from the inland mountainous zone at an elevation of 1066 m.a.s.l and flow through fertile agricultural plains, ultimately reaching the Mediterranean Sea (Fig. 1). The prevailing climate in the Messinia region is relatively humid with an aridity index of 0.78, annual precipitation of 696 mm, mean temperature of 18°C and mean annual potential evaporation of 889 mm (Ekstedt, 2013). These climatic conditions, combined with diverse topography, shape the hydrological processes and agricultural practices of the region. Messinia's hot, dry summers and mild, wet winters are shaped by its distinctive topography of coastal plains and mountainous regions (Kakkavou et al., 2024). The region's varied landscape creates diverse weather patterns, resulting in multiple microclimates (Kalabokidis et al., 2015). These microclimatic variations play a crucial role in determining agricultural practices and have a significant impact on the phenology, growth stages and productivity of olive trees. Elevation variations play a crucial role in influencing the region's hydrology. The mountainous headwaters contribute to groundwater recharge and surface runoff, supporting streamflow throughout the year. The transition from high-altitude cultivated areas (e.g., olive orchards in hilly terrains) to lower-elevation agricultural plains affects soil moisture availability, erosion potential, and irrigation needs. Higher elevations receive more precipitation, promoting groundwater recharge, while lower areas with flatter terrain are more prone to water deficits, especially during dry periods. The Messinia region is primarily characterized by olive cultivation, which covers approximately 70 % of the landscape (Berg et al., 2018; Ekstedt, 2013). Olive orchards are a key tree crop in Mediterranean and Greek agriculture, thriving in well-drained soils but requiring strategic irrigation management, especially in areas with seasonal water scarcity. Irrigation strongly influences the water balance of the study area, with negative environmental consequences. Over-irrigation impacts both groundwater recharge and surface water flows, reducing the availability of freshwater resources in the surrounding area. This leads to the depletion of groundwater and surface water that normally feeds into the vulnerable Gialova Lagoon (Maneas et al., 2019; Manzoni et al., 2020). Rising irrigation demand during dry months, driven by reduced and irregular rainfall along with higher evaporation rates, threatens the sustainability of olive cultivation. Furthermore, excessive and poorly managed irrigation practices may lead to the overexploitation of water resources (Lankford, 2023; Levidow et al., 2014). Given these factors, the region serves as an ideal setting for hydrological and agricultural research. The SWAT+ model simulations will incorporate these dynamics, allowing decision makers for an assessment of sustainable water management strategies in the context of Mediterranean agroecosystems.

2.2. Research framework

Our research design involves multisite AET calibration and validation using local and global soil data, remote sensing and detailed agricultural management practices to enhance SWAT+ model accuracy (Fig. 2). We compare two RS AET products (MODIS and GLEAM) to determine the most accurate product for hydrological modeling in the Messinia region. In addition, we investigate the contribution of a new high-resolution global soil properties map (DSOLMap; López-Ballesteros et al., 2023) to enhance the performance of the SWAT+ model. The modeling approach used in this study consists of 4 different model configurations calibrated and validated individually for each of the four watersheds. These models are based on combinations of two soil maps, and two AET products in four small watersheds with different characteristics (e.g., land use, soil, total area) of the Messinia region, providing a robust approach for accurate hydrological modeling in data-scarce regions.

2.3. Soil and water assessment tool+

The SWAT model is the most commonly used watershed-scale agro-hydrological model worldwide (Fu et al., 2019). It has been successfully applied in data-scarce regions (Bouizrou et al., 2025; Ferreira et al., 2021; Odusanya et al., 2019), including ungauged watersheds (Gitau and Chaubey, 2010; Srinivasan et al., 2010), and has been extensively used for evapotranspiration simulation using RS data (e.g., Chun et al., 2018; Koltsida and Kallioras, 2022; Parajuli et al., 2018). The SWAT+ model, a fully reconstructed version of the original SWAT, provides a more flexible environment for configuring processes and defining agricultural management practices (Arnold et al., 2018; Bieger et al., 2017). Therefore, it was selected for modeling AET in the four ungauged watersheds of the Messinia region by integrating RS data and

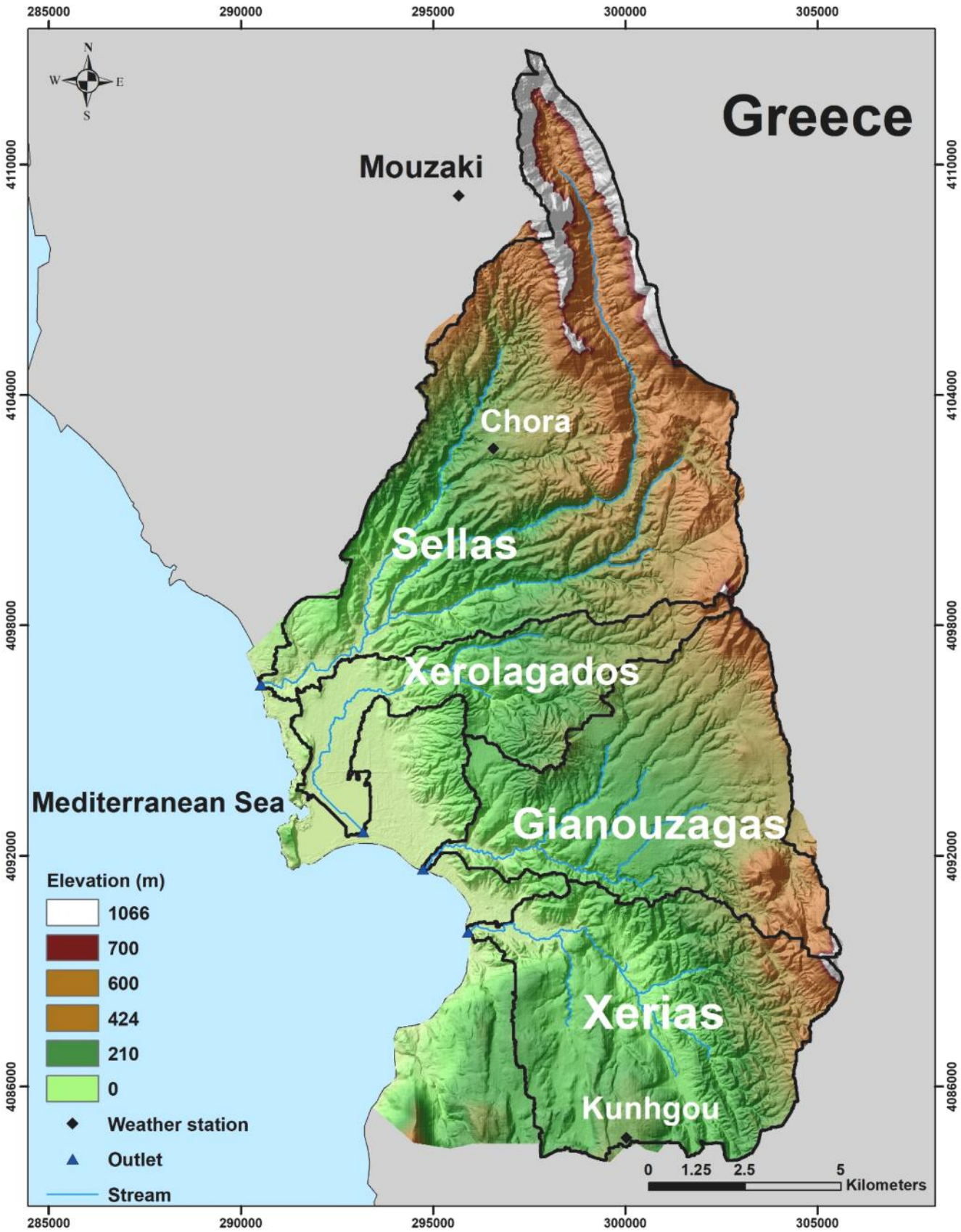

Fig. 1. Map of the Messinia region showing the four watersheds' delineations, the locations of meteorological stations and elevation as a background gradient.

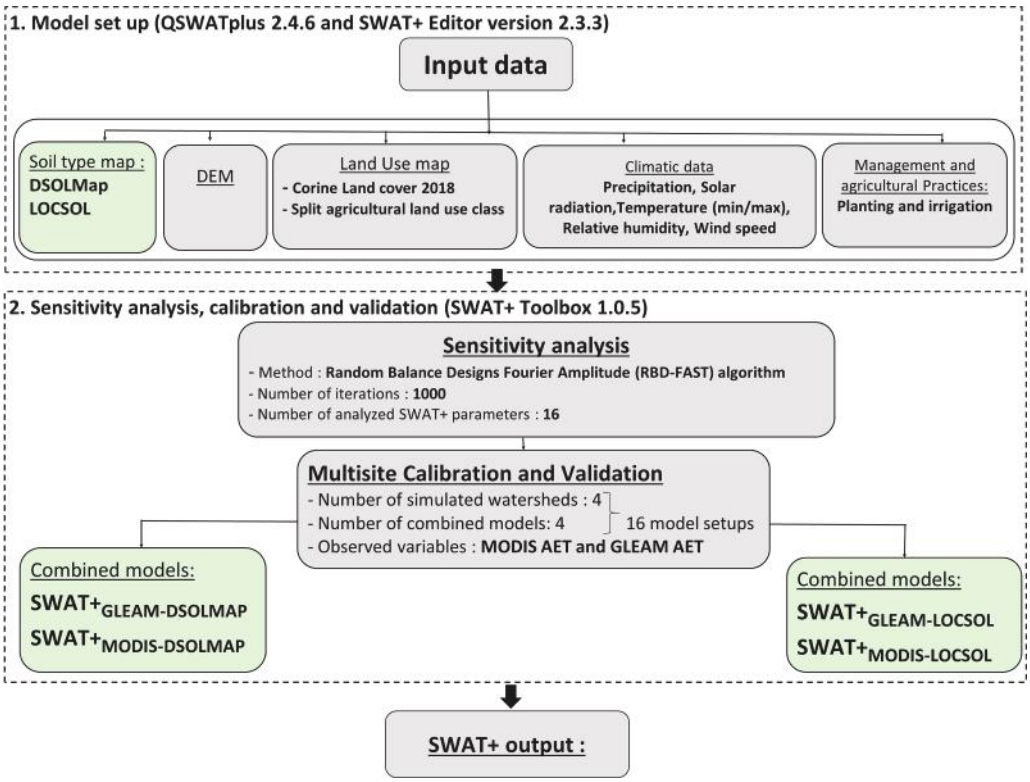

Fig. 2. Research route flowchart illustrating the key steps for SWAT+ modeling in the Messinia region, including data inputs, model setup, and the calibration-validation process.

detailed agricultural management. The model uses daily weather data, including precipitation, relative humidity, temperature (max/min), solar radiation, and wind speed. Operating on a daily timestep, SWAT+ exports output variables such as AET and streamflow at daily, monthly, and yearly timescales. It also incorporates complex conditions and actions within a simple structure, simulating realistic operations through decision tables (Arnold et al., 2018).

In SWAT+ , the simulation of watershed water balance is conceptually divided into two major phases: the land phase and the routing phase (Neitsch et al., 2011). The land phase models hydrological processes occurring on the land surface and within the soil profile, governed by the following water balance equation (Eq. 1):

$$SW_t = SW_0 + \sum_{i=1}^{t}(R_{day} - Q_{surf} - E_a - W_{seep} - Q_{gw}) \quad \text{Eq.1}$$

Where SW_t is the soil water content at time t, 't' is time in days, R_{day} is the daily amount of precipitation, Q_{surf} is the surface runoff, E_a is evapotranspiration, W_{seep} represents the percolation of water from the soil profile into deeper layers, contributing to groundwater recharge and Q_{gw} is the return flow. All units are in mm.

The main hydrological components simulated in the land phase include precipitation, surface runoff, infiltration, evapotranspiration, and groundwater flow. These processes are computed at the level of Hydrological Response Units (HRUs), which represent unique combinations of land use, soil type, and slope. The results are then aggregated at the sub-basin level. Surface runoff at the HRU level can be estimated using one of two methods available in SWAT+ : the Green and Ampt infiltration method (Govindaraju et al., 1996) and the Soil Conservation Service Curve Number (SCS-CN2) method (SCS, 1972). The Green and Ampt method is a physically based infiltration model that can represent infiltration dynamics at daily and sub-daily time scales and is often used for event-based or finer-resolution modeling. The SCS method is an empirical approach developed mainly for daily runoff estimation and is widely used in data scarce regions due to its simplicity and moderate data requirements (Bouizrou et al., 2021; Michaud and Sorooshian, 1994). The routing phase simulates the transport and transformation of water, sediment, nutrients, and other constituents through the stream network from sub-basin outlets to the watershed outlet. SWAT+ offers two routing methods: the Variable Storage method and the Muskingum method, both methods are variations of the Kinematic wave model (Neitsch et al., 2011).

2.4. The estimation of evapotranspiration in SWAT+

SWAT+ simulates AET as the sum of three main components: canopy interception evaporation, plant transpiration, and soil/snow surface evaporation. These components are calculated sequentially each day, constrained by potential evapotranspiration (PET), which acts as an upper limit (Arnold et al., 1998; Bieger et al., 2017; Neitsch et al., 2002, 2005; SWAT+ Gitbook, 2023). PET can be estimated using one of three standard methods: the Penman-Monteith method (Monteith, 1965), the Hargreaves method (Hargreaves and Samani, 1985), or the Priestley-Taylor method (Priestley and Taylor, 1972). In this study, the Penman-Monteith method was selected to estimate PET at the HRU level on a daily time step, as it is the standard recommended by the Food and Agriculture Organization (Allen et al., 1998) and is widely recognized for its accuracy and physical realism, particularly under Mediterranean climatic conditions (Allen et al., 1998; Licciardello et al., 2011).

The calculation of AET in SWAT+ proceeds in a defined sequence. First, intercepted rainfall is removed from the canopy. Next, potential plant transpiration is estimated and adjusted based on soil water availability. Finally, soil evaporation is computed, ensuring that the total of all components does not exceed the PET value. Groundwater contributions to AET may occur indirectly through capillary rise (REVAP) into the root zone (SWAT+ Gitbook, 2023). Additionally, under specific conditions, SWAT+ accounts for other evaporative losses such as sublimation from snow and evaporation from ponded or flooded areas

(SWAT+ Gitbook, 2023). This process-based structure ensures a physically consistent partitioning of water losses based on energy demand, vegetation dynamics, and soil moisture conditions.

2.5. Data description and preparation

To set up and run the SWAT+ model, a variety of spatial datasets are required, including geospatial, climate, and agricultural operations data (Table 1). Daily ground-based meteorological observations, including air temperature, precipitation, relative humidity, wind speed, and solar radiation were collected from three meteorological stations (Chora, Mouzaki, and Kunhgou). The stations along with their corresponding variables and missing data, geographic coordinates, and altitude are summarized in Table 2.

2.5.1. Digital elevation model (DEM)

DEM data, required to derive all topographic attributes at the watershed, sub-basin, and HRU levels was obtained from OpenDEM (OpenDEM Archives, 2023; https://www.opendem.info/archiv_2023.html) at a high spatial resolution of 5 m.

2.5.2. Land use

Land use is an essential dataset for defining and creating HRUs in the SWAT+ model. For this study, land use data was obtained from the CORINE (European Environment Agency, 2021), with a spatial resolution of 100 m. The land use map was rasterized and reclassified into 11 land use classes that are recognized by the SWAT model (Table 3) and included in its database as done in previous studies (Basu et al., 2022; Sertel, 2019; Villani et al., 2024b) (Fig. 3). The dominant agricultural land use class in the four watersheds was further divided into four subclasses based on crop distribution statistics from Ekstedt (2013), considering 70 % olives, 10 % corn, 10 % alfalfa, and 10 % spring wheat, using crop fractions within each watershed of the Messinia region, with the same approach used in Villani et al. (2024a).

Table 1
Details of the data sets used in this study, including variables, time period, and spatial and temporal characteristics.

Data type	Variable	Resolution (m)	Source
Topographic and geospatial data	Digital Elevation (DEM)	5	OpenDEM. (2023) https://asf.alaska.edu/data-sets/sar-data-sets/alos-palsar/)
	Soil	250 5000	The Digital SoiL OpenLand Map (DSOLMap) (López-Ballesteros et al., 2023) (https://www.wateritech.com/data) local soil map (LOCSOL), based on the national soil map
	Land use	100	The Pan-European component of the Copernicus Land Monitoring Service, (European Environment Agency. 2021): (https://land.copernicus.eu/en/products/corine-land-cover)
Climate	P, SLR, TMPmn, TMPmax, RH, WND	Observed	Messinia observatory
	Evapotranspiration (GLEAM)	25000	The Global Land Evaporation Amsterdam Model (GLEAM), (Martens and Miralles,2017) https://www.gleam.eu/
	Evapotranspiration (MODIS)	500	The Evapotranspiration/ Latent Heat Flux product (MODIS), (Running et al., 2021); https://lpdaac.usgs.gov/products/mod16a2v061/
Management and agricultural Practices	Planting, irrigation, and harvesting	-	Living lab and Ekstedt (2013)

Table 2
Characteristics of meteorological stations including location, altitude, meteorological variables, and data availability.

Station	Coordinates	Altitude (m)	Parameter	Missing data (%)
Chora	37.05°N 21.71°E	252 m	Relative humidity	13
			Precipitation	1 >
			Maximum and minimum temperature	13
Mouzaki	37.11°N 21.70°E	426 m	Solar radiation	1 >
			Wind speed	1 >
Kunhgou	36.89°N 21.76°E	253 m	Precipitation	1 >
			Maximum and minimum temperature	8

2.5.3. Soil type

Soil type and its physico-chemical properties are another crucial dataset influencing watershed hydrology by regulating infiltration, runoff, groundwater recharge, and evapotranspiration. Modelers can usually rely on both global datasets with likely inaccurate, yet complete, information and local maps which often have limited information and require the use of pedotransfer functions. By using soil data from two different sources, we assessed the effects of soil data resolution on watershed response. The first one is the Digital Soil Open Land Map (DSOLMap, López-Ballesteros et al., 2023) developed by the OpenGeoHub foundation using a compilation of various data sources. For Greece, the data comes from LUCAS (Land Use and Coverage Area Frame Survey as part of the European Commission's soil survey program) with a high spatial resolution of 250 m. In the study area, a total of six soil types were identified with six layers (Fig. 3). The second soil map (LOCSOL) was developed within the SALAM-MED project based on the national soil map for the Messinia region, which includes eight soil types with one layer (Fig. 3). As part of this project, our research team conducted field measurements of physical and chemical soil properties at

Table 3
Land use classes, their descriptions, and percentages for each watershed within the study area.

SWAT+ code	Description	Percentage (%)			
		Sellas	Xerolagados	Gianouzagas	Xerias
FRST	Forest - Mixed	7.58	3.58	4.36	10.89
FRSD	Forest - Deciduous	7.09	0.95	2.93	0.03
AGRL	Agricultural Land - Generic	32.52	36.7	24.9	56.93
RNGE	Range - Grasses	5.8	-	-	-
RNGB	Range - Brush	3.52	0.34	4.31	22.97
OLIV	Olive groves	41.14	51.95	61.9	6.1
URML	Urban Medium Density	1.1	1.04	1.6	-
UCOM	Commercial	1.25	-	-	1.81
WETW	Water bodies	-	4.04	-	-
WETL	Wetland	-	1.4	-	-
PAST	Pasture	-		-	1.27

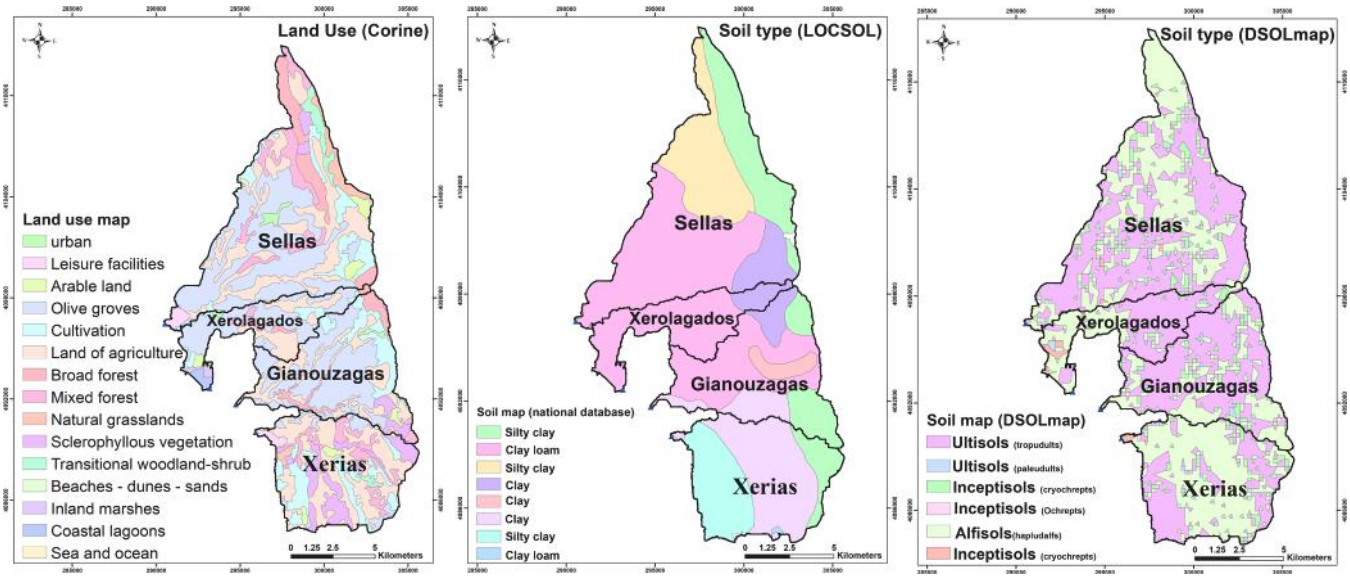

Fig. 3. Land use and soil maps of the Messinia region, including DSOLMap (global soil map) and LOCSOL (locally derived soil map).

three experimental sites within the Messinia Living Lab. At each site, we measured various physical and chemical properties, including layer thickness, sand fractions, silt, clay, coarse fragments, rock fraction, bulk density, moisture, saturated hydraulic conductivity, pH, organic carbon, $CaCO_3$, nitrogen, Mg^{2+}, Na^{+}, K^{+}, and electrical conductivity, with three plots surveyed at each site. These measurements were then used to establish the LOCSOL database, which serves as the soil input for the SWAT+ model. A soil lookup table (CSV file) was created to convert local soil types to SWAT+ soil codes, and the physical and chemical properties for each soil type were compiled into a user soil CSV file for import into SWAT+ . Table 4 lists the required soil parameters and their sources. Key parameters, including electrical conductivity, layer thickness, sand fractions, and bulk density, were derived from the field samples, while others, such as available water capacity and saturated hydraulic conductivity, were obtained from the Soil Water Characteristics model. Rock fragment content and the USLE Soil Erodibility Factor (K) were calculated using pedotransfer functions, as detailed in Supplement 1. The limited number of observation plots (9 in total) used to establish the LOCSOL database may not fully capture the spatial variability of these properties. A larger dataset would be needed to accurately represent soil properties across the region, but gathering such data involves considerable time and associated costs.

Table 4
Soil parameters in LOCSOL soil look up tables.

Parameter	Description	Unit	Source
SOL-Z	Depth from soil surface to bottom of layer	mm	SALAM-MED
SOL_BD	Moist bulk density	$g \cdot cm^{-3}$	Soil Water Characteristics
SOL_AWC	Available water capacity of the soil layer	mm $H_2O \cdot mm^{-1}$	Soil Water Characteristics
SOL_K	Saturated hydraulic conductivity	$mm \cdot hr^{-1}$	Soil Water Characteristics
SOL_CBN	Organic carbon content	% of soil weight	SoilGrids
SOL_CLAY	Clay content	% of soil weight	Soil Water Characteristics
SOL_SILT	Silt content	% of soil weight	Soil Water Characteristics
SOL_SAND	Sand content	% of soil weight	Soil Water Characteristics
ROCK	Rock fragment content	% of total weight	SoilGrids
SAL_ALB	Moist soil albedo	-	Sugathan et al. (2014)
USLE_K	USLE Soil Erodobility Factor (k) factor	metric tons per ($m^3 \times m^2 \times hr$)	Williams (1995)
SOL_EC	Electrical Conductivity	$dS \cdot m^{-1}$	SALAM-MED

2.5.4. Agricultural operation

Incorporating management schedules that include details about irrigation operations, planting, and harvesting is crucial for enhancing model calibration and ensuring consistency between actual and simulated conditions (Faramarzi et al., 2017). For this study, information on crop (plant name) and management schedules, including sowing and harvesting (dates, harvest operation) and irrigation (irrigation type, number of irrigation events, irrigation amount, irrigation dates) operations for each agricultural subclass in each watershed, were obtained from Ekstedt (2013) and the Messinia Living Lab. This information was then integrated into the SWAT+ model using the land management section in the SWAT+ editor. Specifically, sowing dates were set for March 1st for the spring crop (corn) and November 1st for the winter crop (wheat). Irrigation was applied using the sprinkler method at a monthly time step during the summer, starting in May for all crops, and ending in June, July, and October for alfalfa, corn, and olive groves, respectively. Harvest operations were set for September 1st for corn, July 1st for wheat, and November 1st for olive groves.

2.5.5. Remotely sensed evapotranspiration data

The lack of streamflow measurement in the Messinia region led to opting for freely available remote sensing products for multisite calibration and validation of the SWAT+ model. To this end, two commonly used remote sensing AET products (MODIS and GLEAM), characterized by different approaches, algorithms, and spatiotemporal resolutions, were selected and assessed.

MOD16A2 estimates evapotranspiration using thermal infrared signatures from MODIS and daily meteorological reanalysis data (Mu et al., 2011; Mu et al., 2013; Running, 2019). Version 6.1 of the AET dataset is derived from Terra MODIS, a product of the National Aeronautics and Space Administration (NASA). This algorithm uses the Penman-Monteith method to estimate AET based on daily meteorological data and 8-day remote sensing inputs, including land cover, vegetation dynamics, and albedo. For MOD16 algorithm validation, evapotranspiration estimates were compared with tower ET measurements using data from 46 eddy covariance towers and 232 watersheds (Running et al., 2019). The output is an 8-day composite dataset of AET, covering global areas at a spatial resolution of 500 m and includes transpiration from plants, evaporation from moist and wet soil, and rain

intercepted by the canopy. Detailed information about MOD16A2 can be found in Running et al. (2017).

GLEAM estimates evapotranspiration using passive microwave radiation (Martens et al., 2017; Miralles et al., 2011). The GLEAM v3.7 global actual evapotranspiration product is derived from the Global Land Evaporation Amsterdam Model developed by VU University Amsterdam. This model incorporates a set of algorithms to estimate AET from satellite observations based on the modified Priestley and Taylor equation (Priestley and Taylor, 1972). For GLEAM algorithm version 3 validation, a large database consisting of 2325 ground-based soil moisture measurements from sensors and evapotranspiration observations from 91 eddy covariance towers was used. Additionally, analogous datasets derived from GLEAM version 2 were compared with the current version to assess the benefits introduced by the new formulations (Martens et al., 2017). GLEAM generates a daily AET dataset, including soil evaporation, transpiration of short and tall vegetation, evaporation of open water and intercepted rainfall by tall vegetation, with global coverage at a spatial resolution of 0.25°. For further details on the GLEAM dataset, refer to Miralles et al. (2011).

For this study, GLEAM and MODIS products provided AET time series in NetCDF and Raster formats with spatial resolutions of 25000 m and 500 m and temporal resolutions of daily and 8-day, respectively. AET data were extracted for each watershed in the Messinia region using the area-weighted averaging method (Huang et al., 2022; Liu et al., 2016). This method allowed us to derive four distinct AET time series from the MODIS data for each of the four watersheds. However, for the GLEAM data, we obtained only three distinct AET time series as watersheds 3 and 4 showed similar AET values due to the coarse spatial resolution of the GLEAM dataset. Then, monthly AET values were derived by aggregating daily AET data according to the number of days in each month and the corresponding Julian date. For MODIS, the 8-day AET data were aggregated into monthly values by summing three observations per month to obtain the total monthly AET.

Comparison of GLEAM and MODIS with the FAO-56 Penman-Monteith Method

An initial comparison of monthly AET time series sourced from GLEAM and MODIS datasets with an independent estimate of AET was carried out using observed weather data from the three stations. In this estimation, we first computed the daily reference evapotranspiration (ETo) using the FAO-56 Penman-Monteith equation:

$$ET0 = \frac{0.408\Delta(R_n - G) + \gamma \frac{900}{T+273} u_2 (e_\delta - e_\alpha)}{\Delta + \gamma(1 + 0.34u_2)} \quad \text{Eq.2}$$

Where R_n is the net radiation (MJ/m^2/day), G is the soil heat flux density (MJ/m^2/day), T is the mean daily air temperature (°C), u_2 is the wind speed at 2 m height (m/s), e_s is the saturation vapor pressure (kPa), e_a is the actual vapor pressure (kPa), Δ is the slope of the vapor pressure curve (kPa/°C), and γ is the psychrometric constant (kPa/°C).

A weighted averaging approach was used to compute the final crop coefficient (Kc) for the Messinia region, taking into account the weight and Kc values from FAO (1998) for the three main land uses. For olive trees which dominate the region, the Kc value of 0.7 was applied with a weight of 0.7. For rangeland with a Kc value of 0.5 and a weight of 0.15, and for forest areas where the Kc value is also 0.7 with a weight of 0.15, the contributions were calculated accordingly. The final Kc value, derived from the weighted average of these land use types was 0.67, reflecting the overall water demand across the region.

Once ETo was computed, daily AET was then estimated based on the crop coefficient using the following equation:

$$AET = K_c \times ET_0 \quad \text{Eq.3}$$

Finally, the estimated AET was compared with GLEAM and MODIS datasets using the monthly mean trends for the study period. The Python programming language was used to compute the daily ETo, AET, and the aggregated monthly AET.

2.6. Model setup and configuration

Agro-hydrological modeling of the four watersheds in the Messinia region was conducted using three SWAT+ related interfaces. We used the QSWAT+ (version 2.4.6) plugin, based on the long-term release of QGIS (version 3.28.11), to set up the four watersheds, including the processing of topographic and geospatial data, as well as management and agricultural practices (planting, irrigation, and harvesting), as illustrated in Table 1. This initial setup of the SWAT+ model included DEM, land use, and soil type, which were prepared to automatically complete stream parameterization, watershed delineation, and HRU creation. In addition, the agricultural land use was further divided into subclasses to better represent agriculture in the SWAT+ model.

Watershed delineation was carried out using threshold values of 18 km^2 for channels and 180 km^2 for streams, which allowed for a realistic depiction of the drainage network. The watershed delineation resulted in a model setup with 9 subbasins and 95 channels for the Sellas watershed; 3 subbasins and 27 channels for the Xerolagados watershed; 7 subbasins and 49 channels for the Gianouzagas watershed; and 9 subbasins and 67 channels for the Xerias watershed. HRUs were created by overlaying land use, soil type, and slope. The DEM was reclassified into two slope classes: 0–7 % to represent gently to moderately sloping land, and over 7 % to represent steep areas. We selected the 'filter by area' method for HRU definition, with the area threshold set to 0 %, including all possible HRUs in the model. This resulted in 3381, 903, 1067, and 2812 HRUs for the Sellas, Xerolagados, Gianouzagas, and Xerias watersheds, respectively.

To address missing data, SWAT+ incorporates the WGEN statistical weather generator module, which generates synthetic weather data when observed measurements are unavailable (Neitsch et al., 2011). WGEN models the spatiotemporal dynamics of observed weather variables and requires monthly statistics for temperature (maximum, minimum, dew point), precipitation (average, skewness), solar radiation, and wind speed. The SWAT Weather Database tool (Essenfelder, 2016) was used to store and generate inputs for the SWAT+ model and to calculate WGEN statistics from daily weather data.

Next, the SWAT+ Editor (version 2.3.3) was used to edit and complete the models for the Messinia region. Precipitation for each subbasin in SWAT+ was sourced from the nearest station using the Nearest Neighbor method, and missing climate data in the Messinia region (Table 2) were filled using SWAT WGEN. In this study, we selected the SCS Curve Number II method for runoff estimation (SCS, 1972), the Penman-Monteith equation for evapotranspiration (Monteith, 1965; Penman, 1956), and the Variable Storage method for channel water routing. Finally, we used the SWAT+ Toolbox (version 1.0) to perform automatic sensitivity analysis, calibration, and validation for monthly AET.

2.7. Sensitivity analysis, calibration and validation

The successful application of highly parameterized models relies on sensitivity analysis (SA), calibration and validation (Abbaspour et al., 2015; Arnold et al., 2012). As a physically-based model, SWAT+ can simulate a wide range of hydrological processes, including water quality and quantity variables and involves a large number of parameters (184) to be calibrated or specified. Focusing on highly sensitive parameters improves the estimation of model values and reduces uncertainty (Lenhart et al., 2002). Given the large number of parameters for SA and calibration, a preselection based on the literature was conducted to identify those most influential on the water cycle, particularly AET simulated by SWAT+ . In this study, we selected 16 parameters identified in previous studies (Jiménez-Navarro et al., 2024; López-Ballesteros et al., 2019; López-Ramírez et al., 2021; Mohammadi et al., 2021; Odusanya et al., 2019) as sensitive to both evapotranspiration and streamflow for SA. The SWAT+ Toolbox is an open-access, free graphical user interface belonging to the SWAT+ community tools (https://

swat.tamu.edu/software/plus/). It has been widely used in recent studies for sensitivity analysis (e.g., Kardhana et al., 2024; Pulighe et al., 2021; Villani et al., 2024a; Yulianti et al., 2025) and was selected for the SA, calibration, and validation processes. The sensitive parameters for four watersheds in the Messinia region were identified using the Random Balance Designs Fourier Amplitude (RBD-FAST) algorithm (Tarantola et al., 2006). By performing one complete iteration of 1000 simulations for a combined model configuration, the t-statistic was used as a statistical indicator to identify parameters considered sensitive with large t-stat values.

The next step in the calibration and validation process is to calibrate the most sensitive parameters identified through sensitivity analysis. To this end, the SWAT+ combined models were continuously calibrated and validated using a 10-year period of monthly RS-ET data at watershed scale based on a multisite calibration approach. The choice of the length of the study period was determined by the availability of daily weather input data for the SWAT+ model (minimum and maximum temperature, relative humidity, solar radiation, precipitation, and wind speed) over a 10-year period. Furthermore, we analyzed the interannual variability of the different SWAT input weather variables using the coefficient of variation (COV). The COV values for each parameter indicate the level of variability in relation to the mean. According to Asfaw et al. (2018), COV is used to classify rainfall variability as low (COV < 20 %), moderate (20 % < COV < 30 %), and high (COV > 30 %). The results revealed low variation in wind speed (6 %), minimum and maximum temperature (8.90 % and 18 %, respectively), precipitation (4 %), and humidity (13 %), with moderate variation in solar radiation (30 %). Given the low interannual variability of the relevant variables for the SWAT model, we consider a 10-year simulation period to be sufficient for calibration and validation purposes, as it adequately represents the hydrological processes in the Messinia region, where climate conditions were relatively stable during this period.

The traditional split-sample strategy (Klemeš, 1986) was adopted by dividing the entire study period into two sub-periods: the first period (2015–2018) was used for model calibration, and the remaining sub-period (2019–2022) was used for validation, assessing the calibrated models' ability to accurately simulate evapotranspiration in the four watersheds. The first two years (2013–2014) were considered as a warm-up period for model initialization and to reduce uncertainty related to initial conditions. Automatic calibration was carried out by SWAT+ toolbox using the Dynamic Dimensional Search (DDS) method on 16 combined models. The DDS algorithm is a stochastic, single-solution global search method designed to find good global solutions within a specified model evaluation limit by exploring the range of user-defined parameter values between the minimum and maximum. It is well-suited for calibrating models with many parameters and is particularly effective for computationally demanding optimization problems, such as the calibration of distributed hydrological models (Tolson and Shoemaker, 2007). 600 simulations were run per iteration, resulting in a total of 9600 simulations during the calibration phase. After completing 600 runs (1 iteration) for each model, the model displayed the best set of calibrated parameters that provided the most accurate results based on performance criteria (best simulation). The optimal values of the calibrated parameters for each combined model in each watershed were then used for validation, without any further adjustments to the model parameters.

2.8. Model performance evaluation

The performance of all combined models was evaluated using both statistical and graphical methods. Four common indices were used: Nash-Sutcliffe efficiency (NSE) and R^2 assessed the goodness of fit between simulated and observed AET values. The ratio of root mean square error to the standard deviation of observed data (RSR) and percent bias (PBIAS) were used to quantify discrepancies between model predictions and observed RS AET. According to Moriasi et al. (2015a), model performance related to streamflow simulation is considered satisfactory when NSE > 0.5 and PBIAS < ±15 %. Additionally, Moriasi et al. (2007) suggest that RSR < 0.7 and R^2 > 0.6 are acceptable thresholds (Table 5). In this study, we applied the same performance criteria guidelines for AET simulation as used in previous studies (e.g., Koltsida and Kallioras, 2022; Odusanya et al., 2019). Graphical evaluation included scatter plots, box plots and maps to further assess model performance.

3. Results

3.1. Intercomparison of AET estimates from GLEAM, MODIS, and the FAO-56 P-M

The monthly mean AET values computed using the FAO-56 P-M method, along with MODIS and GLEAM AET were compared for the Messinia region over 2013–2022. As shown in Fig. 4, MODIS AET tends to be lower, especially in summer, whereas GLEAM and FAO-56 P-M estimates are higher and more closely aligned. Scatter plots in Fig. 4, further illustrate this by showing a strong correlation between GLEAM and FAO-56 P-M ($R^2 = 0.91$), with tight clustering along the regression line. In contrast, MODIS AET is more scattered and falls below the 1:1 line ($R^2 = 0.59$), confirming its underestimation and inconsistencies with FAO-56 P–M. This comparison highlights substantial differences between MODIS and GLEAM datasets, with GLEAM more closely matching FAO-56 P-M AET estimates in the Messinia region.

3.2. Sensitivity analysis

The relative sensitivity value, group and ranking of the 16 preselected parameters are depicted in Table 6. The table shows the six most sensitive parameters with higher t-stat values meaning greater sensitivity. Our results indicate that the soil-related parameters available water capacity (AWC) and soil bulk density (BD) are the most sensitive with t-stat values of 0.72 and 0.08, respectively. Other sensitive parameters, including curve number 2 (CN2), curve number 3 (CN3_SWF), percolation coefficient (PERCO) and plant uptake compensation factor (EPCO), had t-stat values ranging from 0.025 to 0.057. The SA results highlight the influence of soil and vegetation parameters in shaping hydrological processes in the Messinia region, dominated by olive plantations. N'guessan et al. (2024) and Sánchez-Gómez et al. (2024) found similar results and identified these parameters as sensitive to watershed evapotranspiration in the SWAT+ model. Therefore, these six parameters were considered for calibration.

3.3. Performance assessment of the models

3.3.1. Calibration phase

The six most influential SWAT+ model parameters for the Messinia region were used to calibrate AET (retrieved from GLEAM and MODIS) using DSOLMap and LOCSOL soil inputs. The performance assessment using the goodness-of-fit criteria NSE and R^2 is presented in Figs. 5, 6 and Table S2 in the Online Supplementary Material. The Fig. 5 illustrates

Table 5
Performance criteria from Moriasi et al. (2007), (2015) used for assessing remotely sensed actual evapotranspiration in the Messinia region.

Performance rating	NSE	RSR	PBIAS (%)	R^2
Very good	0.75 < NSE ≤ 1.00	0.00 ≤ RSR ≤ 0.50	PBIAS ≤ ±3.0	0.80 ≤ R^2 < 0.90
Good	0.65 < NSE ≤ 0.75	0.50 < RSR ≤ 0.60	±3.0 < PBIAS < ±10	0.70 ≤ R^2 < 0.80
Satisfactory	0.50 < NSE ≤ 0.65	0.60 < RSR ≤ 0.70	±10 ≤ PBIAS ≤ ±15	0.6 ≤ R^2 < 0.70
Unsatisfactory	NSE ≤ 0.50	RSR > 0.70	PBIAS ≥ ±15	R^2 < 0.6

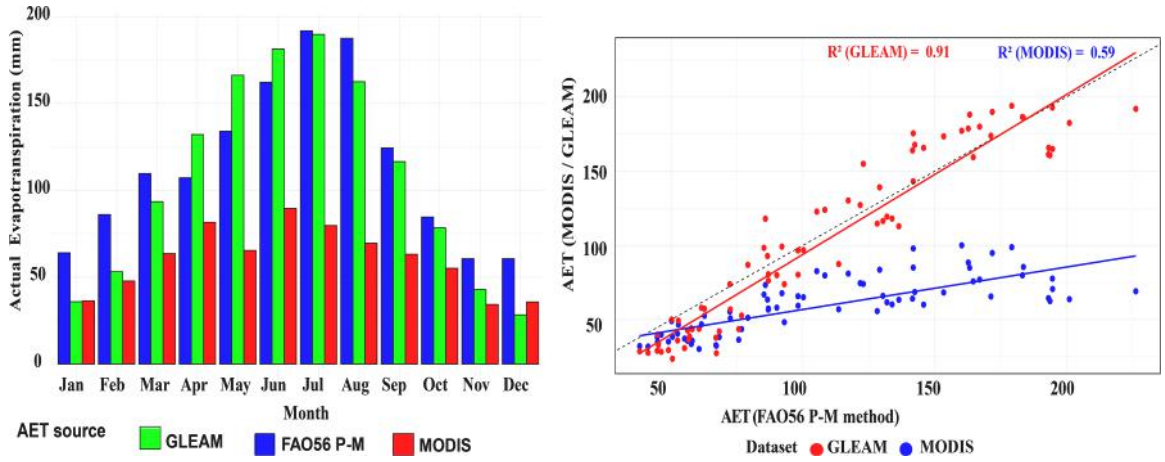

Fig. 4. Scatter plot and bar graph of the monthly mean AET values computed using the FAO-56 P-M method, along with MODIS and GLEAM AET data for the Messinia region from 2013 to 2022.

Table 6
Sensitive parameters and their t-stat values for actual evapotranspiration using the SWAT+ Toolbox.

Group	Change type	Parameter	Unit	t-stat
sol	Relative	awc	mm_H20/mm	0.7149
sol	Relative	bd	Mg/m**3	0.0808
hru	Replace	epco	-	0.0563
hru	Replace	cn3_swf	-	0.0265
hru	Replace	perco	fraction	0.0251
hru	Percent	cn2		0.0144

Note: 'Relative' refers to a relative change in the initial value of the model parameter, 'Replace' refers to the replacement of the initial parameter value, and 'Percent' refers to an absolute percentage increase in the initial parameter value.

the variation in NSE values during the calibration and validation phases using both RS AET products and two soil map sources. Each boxplot represents the NSE values obtained by each combined model across the four watersheds of the Messinia region. The lower and upper bounds of each box correspond to the 25th and 75th percentiles, the horizontal line represents the median and the red dot represents the mean. The figure shows that the combined models do not have identical performances. Specifically, it demonstrates that based on the Nash values obtained during calibration, the SWAT+ model using AET from GLEAM clearly outperforms SWAT+ using AET from MODIS. This is evidenced by a smaller variation in NSE values across the Messinia region with tighter boxplots and higher mean NSE values of 0.75 and 0.71 for SWAT+-$_{\text{GLEAM\_DSOLMap}}$ and SWAT+$_{\text{GLEAM\_LOCSOL}}$, respectively. In contrast, SWAT+$_{\text{MODIS\_DSOLMap}}$ and SWAT+$_{\text{MODIS\_LOCSOL}}$ had mean NSE values of 0.55 and 0.25, respectively, with greater performance variation from watershed to watershed.

Among the four calibrated models, SWAT+$_{\text{GLEAM\_DSOLMap}}$ exhibited very good performance, with NSE values ranging from 0.62 to 0.81. SWAT+$_{\text{GLEAM\_LOCSOL}}$ demonstrated overall good performance, with NSE values between 0.23 and 0.87. SWAT+$_{\text{MODIS\_DSOLMap}}$ achieved satisfactory performance, with NSE values ranging from 0.37 to 0.73, while SWAT+$_{\text{MODIS\_LOCSOL}}$ showed the lowest performance, with NSE values between −0.12 and 0.65 (Table S2). Furthermore, Fig. 6 shows scatter plots of monthly GLEAM and MODIS based AET versus SWAT+ simulated AET for the four watersheds in the Messinia region using DSOLMap and LOCSOL soil data. During calibration, SWAT+ estimated AET exhibited a strong linear correlation with GLEAM based AET in the four watersheds, with R^2 values ranging from 0.74 to 0.92. The regression line slope for all models with both soil inputs was close to one, confirming the positive linear relationship between SWAT+ simulated and GLEAM AET. In contrast, the SWAT+ model showed a weak relationship with the MODIS based AET in the Xerolagados, Gianouzagas, and Xerias watersheds, with R^2 values ranging from 0.13 to 0.63.

The PBIAS and RSR criteria were used to measure discrepancies between model predictions and observed evapotranspiration estimates (Figs. 7 and 8). Fig. 7 shows the watershed-level PBIAS scores for evapotranspiration simulation by SWAT+ using different soil data

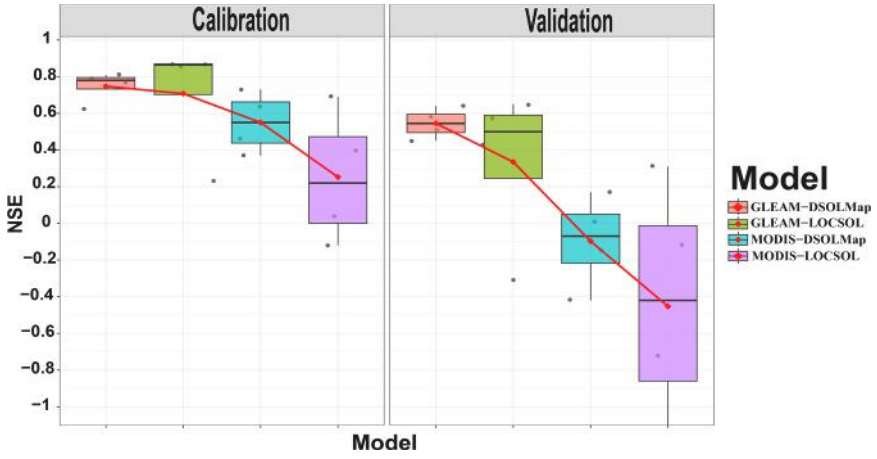

Fig. 5. Box plots of the Nash-Sutcliffe Efficiency (NSE) criterion for the calibration and validation of evapotranspiration across the four Messinia region watersheds.

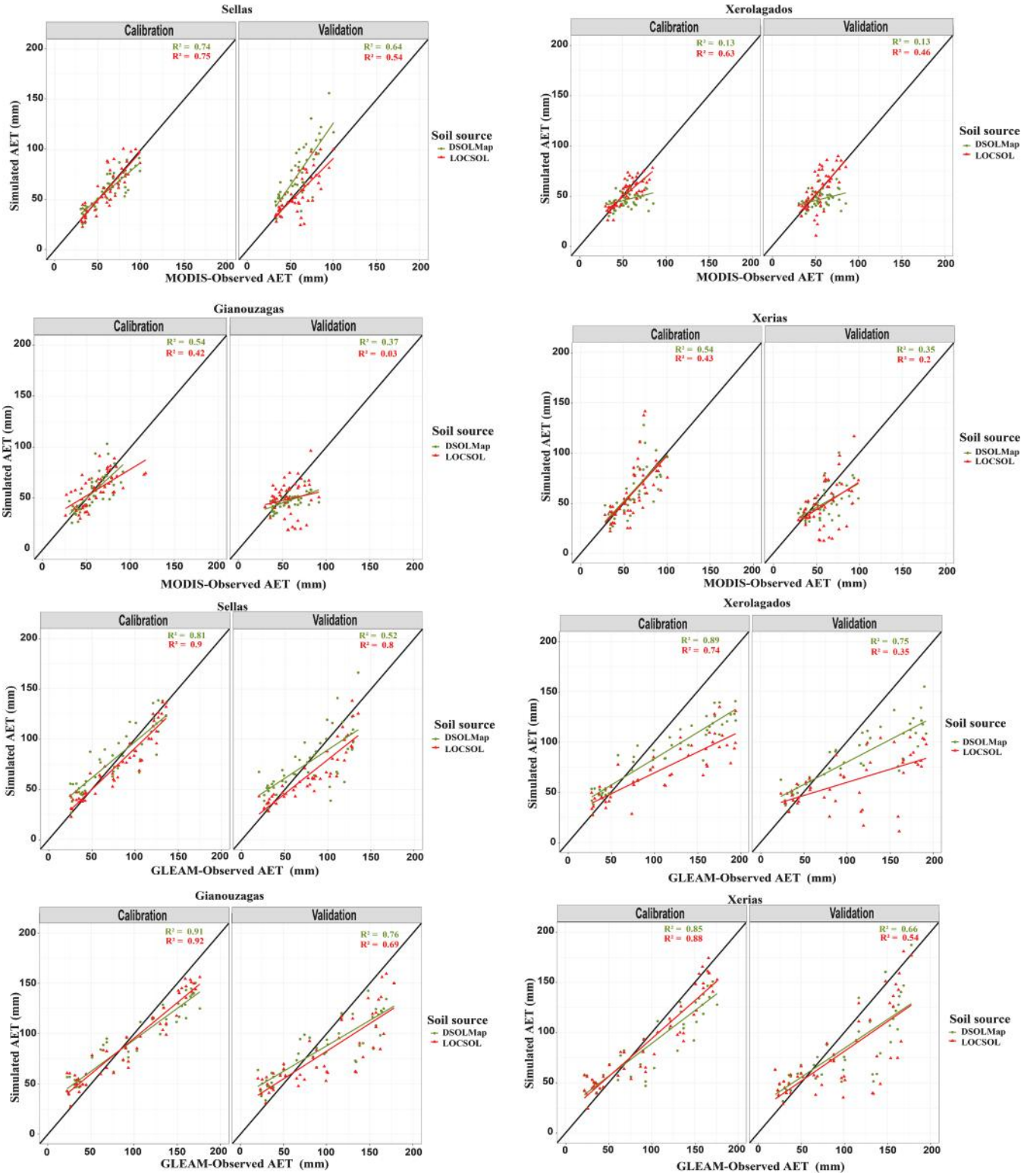

Fig. 6. Scatter plots of observed and simulated evapotranspiration for the four Messinia region watersheds using DSOLMap and LOCSOL soil data.

during calibration and validation. The spatial analysis of PBIAS values during calibration indicates that the SWAT+ simulations demonstrated satisfactory performance for fourteen combined models, with values falling within the range of PBIAS $< \pm 15$ % out of the sixteen combined models. Among these, twelve yielded positive PBIAS values of less than 9.5 % during the calibration period. This indicates good to very good performances achieved by the models. The two combined models that exhibited unsatisfactory performance are those simulating GLEAM AET in Xerolagados, the smallest watershed in the Messenia region. During calibration, RSR values (Fig. 8) indicated that six out of eight model combinations using GLEAM AET data achieved very good performance (RSR < 0.5). The two combinations that performed unsatisfactorily were those simulating AET in the Xerolagados watershed. In contrast, five out of eight combinations using MODIS AET data had unsatisfactory

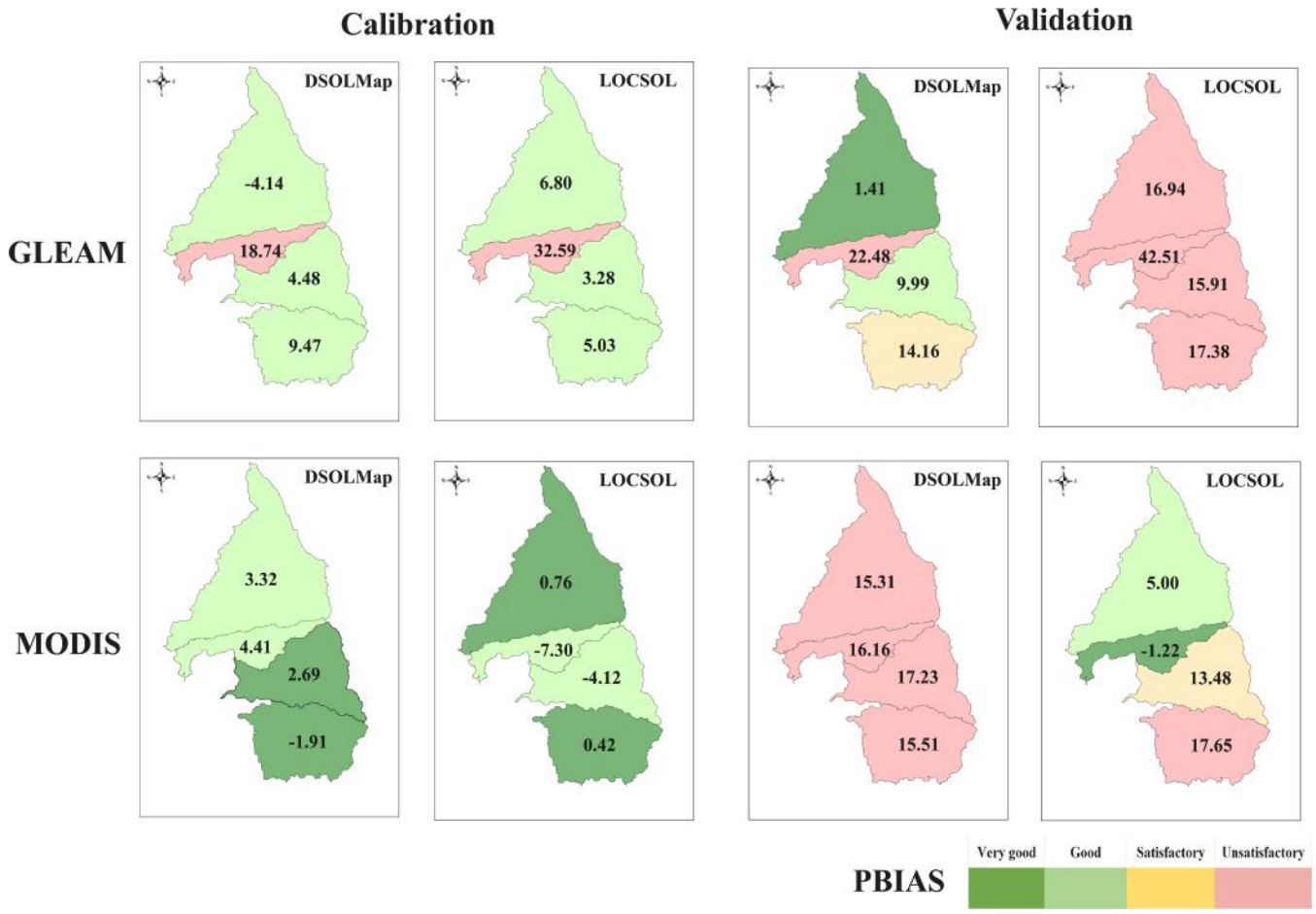

Fig. 7. Watershed-level PBIAS values for evapotranspiration simulation by SWAT+ using different soil data during calibration and validation.

performance, with RSR values greater than 0.7, highlighting the outperformance of GLEAM over MODIS.

The visual inspection of simulated versus observed RS AET was used to further evaluate the models' performance in calibration period. Fig. 9 shows the graphical comparison of simulated and measured monthly AET values for the calibration period across different combined models for four watersheds. It can be observed that the SWAT+ simulated AET satisfactorily reproduced the temporal variation, magnitude and peaks of AET estimated by both RS AET products in the SELLAS, Gianouzagas, and Xerias watersheds, particularly when combining GLEAM AET and DSOLMap as the soil data input source. However, the model failed to accurately reproduce the AET in the Xerolagados watershed, particularly the peak values corresponding to the summer period, especially when using local soil conditions (LOCSOL) as the model soil input.

3.3.2. *Validation phase*

The boxplots in Fig. 5 confirm that SWAT+$_{\text{GLEAM-DSOLMap}}$ is the best combination, demonstrating satisfactory performance in the validation phase, with low NSE variation across the region and a mean NSE of 0.55. The worst performance by the SWAT+ model occurred when using MODIS as the AET data source, with negative mean NSE values and high variation across watersheds. In more detail, the Table S2 shows that the NSE values for SWAT+$_{\text{GLEAM-DSOLMap}}$ were 0.51, 0.45, 0.64, and 0.58 for the Sellas, Xerolagados, Gianouzagas, and Xerias watersheds. The SWAT+$_{\text{GLEAM-LOCSOL}}$ model achieved satisfactory performance in the Sellas (NSE = 0.65) and Gianouzagas (NSE = 0.57) watersheds but showed unsatisfactory performance in the Xerolagados and Xerias watersheds (NSE < 0.5). All MODIS simulations had NSE values below 0.5, indicating unsatisfactory performance. The scatter plots of AET from the SWAT+ model versus GLEAM AET when using DSOLMap as the soil input, exhibited a good linear correlation in the four watersheds, with the slope of the regression line being closer to 1 compared to when using LOCSOL as the soil input (Fig. 6). In addition, MODIS AET demonstrated a weak relationship with SWAT+ simulated AET for all watersheds when using both soil map sources. The R^2 criterion showed similar trends, with the SWAT+$_{\text{GLEAM-DSOLMap}}$ model achieving the best performance, scoring R^2 values of 0.52, 0.75, 0.76 and 0.66 for the Sellas, Xerolagados, Gianouzagas and Xerias watersheds, respectively (Fig. 6). The SWAT+$_{\text{GLEAM-LOCSOL}}$ model came in second with satisfactory R^2 values of 0.80 and 0.69 for the Sellas and Gianouzagas watersheds, respectively. The same model performed unsatisfactorily in the Xerolagados ($R^2 = 0.35$) and Xerias ($R^2 = 0.54$) watersheds. The SWAT+$_{\text{MODIS-DSOLMap}}$ and SWAT+$_{\text{MODIS-LOCSOL}}$ models showed unsatisfactory performance with R^2 values below 0.6.

As shown in Fig. 7, only 38 % of the models performed satisfactorily to very good. Similar to the calibration phase, the SWAT+$_{\text{GLEAM_DSOLMap}}$ model achieved satisfactory performance in the Sellas (PBIAS = 1.41), Gianouzagas (PBIAS = 9.99), and Xerias (PBIAS = 14.16) watersheds but continued to perform unsatisfactorily in the Xerolagados watershed (PBIAS = 22.48). Additionally, the SWAT+$_{\text{MODIS_LOCSOL}}$ model achieved satisfactory performance in the Sellas (PBIAS = 5), Xerolagados (PBIAS = −1.22), and Gianouzagas (PBIAS = 13.48) watersheds but showed unsatisfactory performance in the Xerias watershed (PBIAS = 17.65). Similar to calibration, watershed-level RSR values show that six out of eight model combinations using GLEAM achieved satisfactory to good performance (RSR ≤ 0.7), while all models using MODIS failed to meet satisfactory performance (RSR ≥ 0.7) (Fig. 8).

Fig. 9 compares the simulated and observed AET time series over the

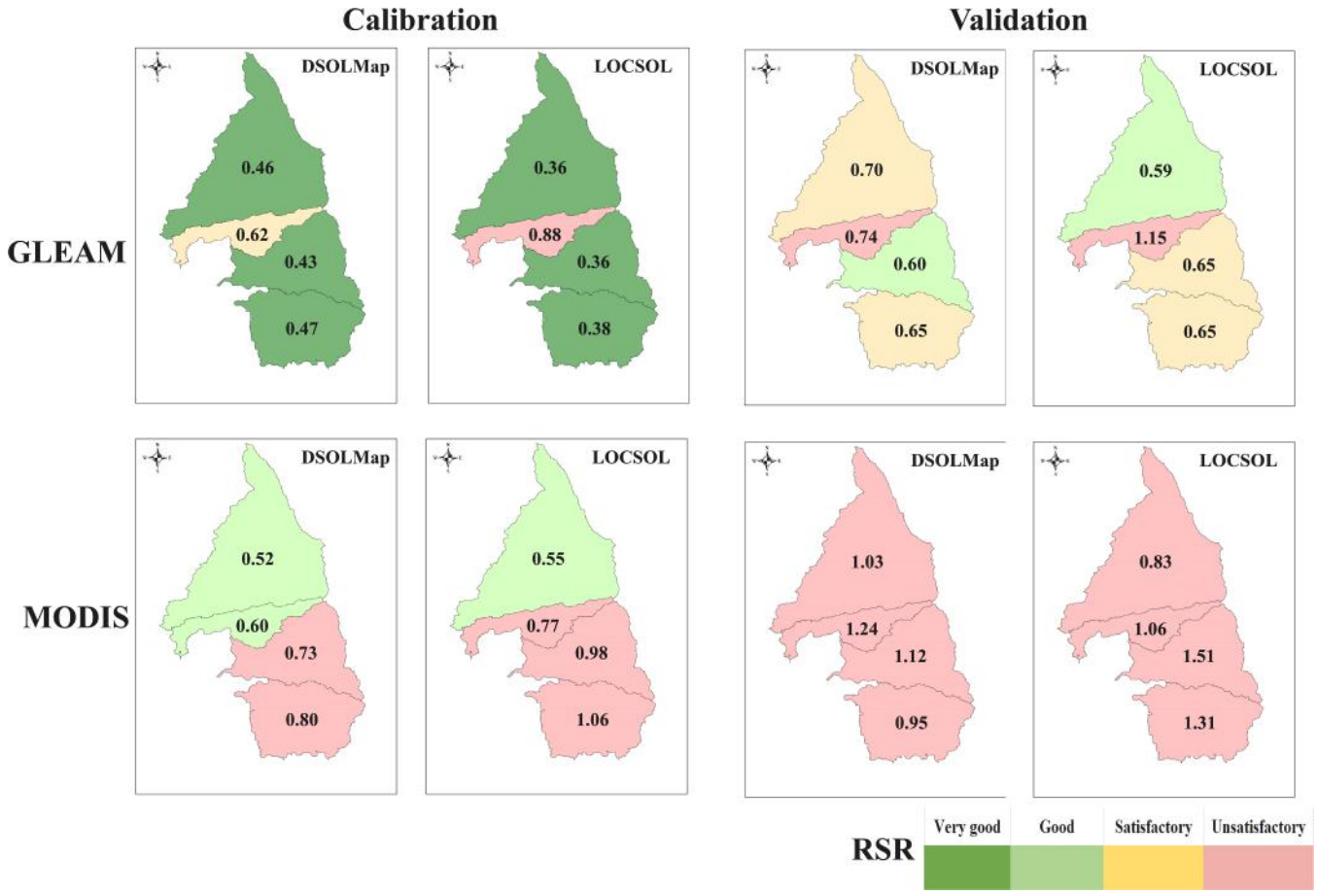

Fig. 8. Watershed-level RSR values from evapotranspiration simulations using DSOLMap and LOCSOL soil data with SWAT+ during calibration and validation.

validation period. It shows that the SWAT+ model exhibits slight degradation in performance. Both GLEAM and MODIS AET values, especially when combined with DSOLMap, were satisfactorily reproduced in the Sellas and Xerias watersheds, in terms of magnitude and peaks during the dry summer season. However, the model failed to accurately simulate AET values in the Gianouzagas and Xerolagados watersheds, particularly regarding peak values.

SWAT+ model performance analysis shows that models integrating high-resolution global soil maps performed better than models that integrate local soil maps in the Messinia region during calibration and validation phases (Figs. 5, 6, 7, 8, 9). Moreover, models that used GLEAM AET data achieved better results than those using MODIS AET data, suggesting improved performance in both calibration and validation. The combination of DSOLMap and GLEAM AET soil data was the only setup that achieved satisfactory performance (NSE $>$ 0.5) in all watersheds. This indicates that SWAT+ models were more successful in capturing GLEAM AET than MODIS AET, whatever the soil type used, in all four watersheds.

3.3.3. *Water balance components simulated by the SWAT+ model*

Table 7 displays the mean annual values of the main water balance components simulated by the best-calibrated model (SWAT+-$_{\text{GLEAM\_DSOLMap}}$) in the four watersheds of Messinia over the entire period. Mean annual precipitation varies across watersheds but tends to decrease with latitude, with the southernmost watershed (Xerias) receiving the highest rainfall (1044 mm) and the northernmost (Sellas) receiving the lowest (769 mm) (Table 7). In addition, total irrigation varies among the watersheds, with estimated values of 181 mm, 272 mm, 160 mm, and 77 mm for Sellas, Xerolagados, Gianouzagas, and Xerias, respectively. The highest irrigation values are observed in Sellas and Xerolagados, which have the largest percentage of olive crops.

3.3.4. *Model performance according to the characteristics of watersheds*

The results of AET simulations using different SWAT+ model configurations were evaluated further to assess the effects of land use types and watershed size on model performance. Results were found to vary with watershed characteristics with the best overall performance in the larger watersheds (Sellas = 90 km^2, Gianouzagas = 47 km^2, Xerias = 48 km^2) compared to the smaller Xerolagados watershed (25 km^2). Considering the land use characteristics, Xerolagados, which has the highest percentage of agricultural land (89 %) and is the only watershed with water bodies and wetlands (5.44 %) (Table 3), was the only watershed where SWAT+ failed to be validated. This failure is likely due to the challenges in accurately representing AET in a watershed dominated by agricultural land, particularly olive cultivation, which can have complex water and evapotranspiration dynamics.

The proposed modeling approach, integrating remote sensing data, high-resolution soil maps, and management schedules in the SWAT+ model, provides useful insights for improving water resource management in Messinia. The validated model serves as a foundation for assessing climate change impacts on water availability and guiding adaptive management strategies. The variability in AET and irrigation demand across watersheds underscores the need for site-specific irrigation strategies to enhance water efficiency in Messinia's agriculture-dominated landscape. Model performance varies with watershed characteristics, such as agricultural land extent and water bodies, highlighting the need for tailored water management approaches.

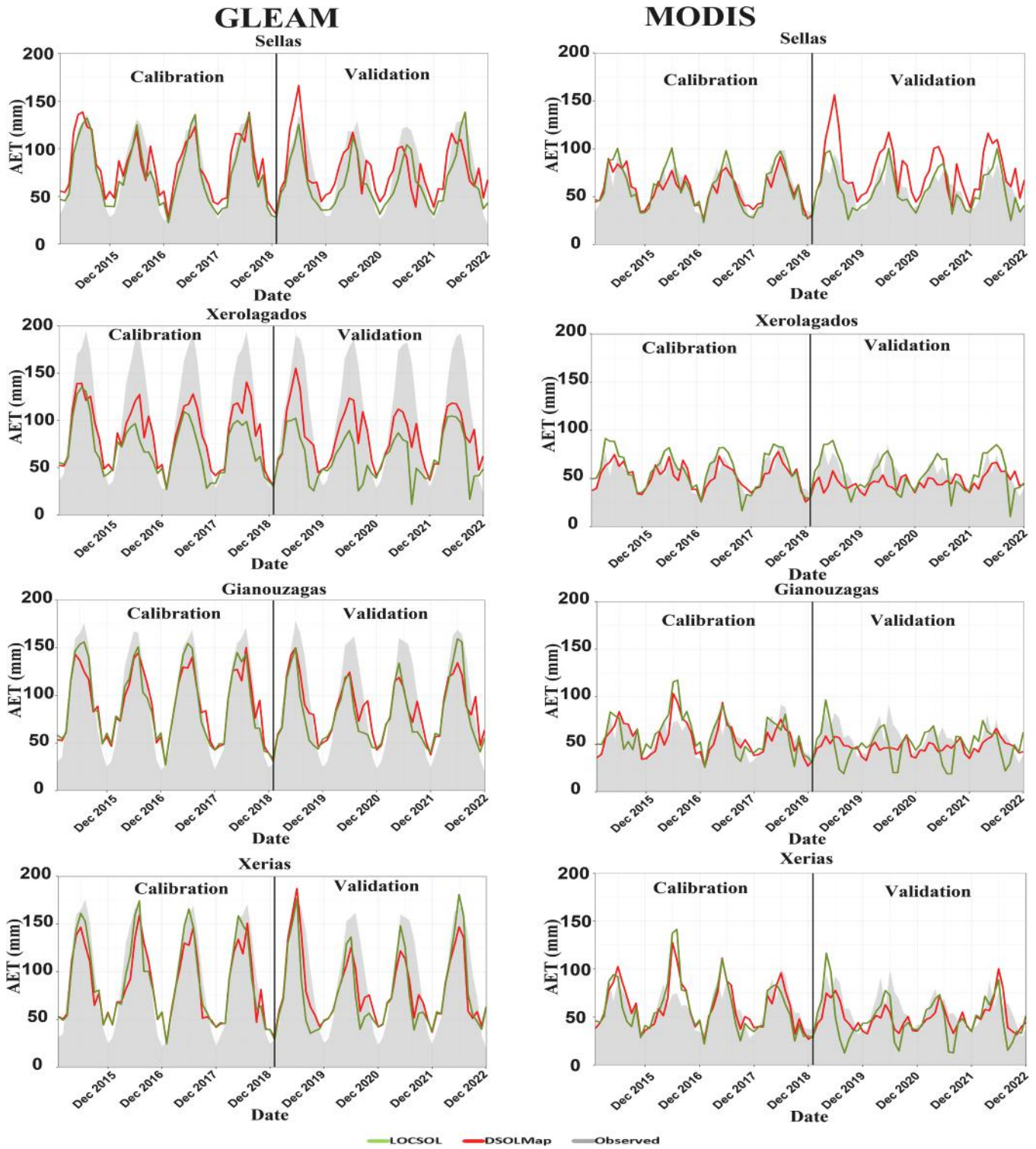

Fig. 9. Observed and simulated evapotranspiration for the four Messinia region watersheds using different soil data with the SWAT+ model during calibration and validation.

4. Discussion

4.1. Sensitivity of SWAT+ parameters to evapotranspiration in the Messinia region

In the Messinia region, AWC and BD were the most sensitive parameters influencing AET. The high sensitivity of soil AWC regulates soil moisture and plant growth (USDA, 2005) and governs water availability for plant uptake and evapotranspiration (Abiy et al., 2019). As AWC increases, evapotranspiration from both soil and canopy also rises due to greater soil moisture availability to plants. Similarly, soil BD affects soil porosity and infiltration, with changes in BD influencing water partitioning between evapotranspiration, infiltration, and runoff generation (Shi et al., 2022). Similar findings were reported by Koltsida and Kallioras (2022), Moriasi et al. (2015b) and Sirisena et al. (2020), who also found soil-related parameters to be very sensitive for AET simulations

Table 7
Annual mean values of water balance components (evapotranspiration, precipitation, and irrigation) across the four watersheds in the Messinia region.

Watershed	Precipitation (mm)	AET (mm)	Irrigation (mm)
Sellas	769	927	181
Xerolagados	770	554	272
Gianouzagas	900	570	160
Xerias	1044	733	77

using SWAT and SWAT+ models. The sensitivity of EPCO further highlights the importance of vegetation by regulating the water balance, as it governs plant ET by controlling water uptake from different layers within the rooting zone. As EPCO increases, it allows the plant to extract more water from deeper soil layers (Wu and Johnston, 2007). Olive trees, with their deep-rooted systems, significantly influence sensitive parameters such as AWC, EPCO, and BD by enhancing water uptake from deeper soil layers, thus increasing evapotranspiration and improving water retention. Other sensitive parameters, including CN2, PERCO, and CN3_SWF, depend on soil permeability, initial soil moisture condition, and land use, and govern surface runoff (CN2) and evapotranspiration (CN3_SWF). Jiménez-Navarro et al. (2024) found that parameters such as CN2, EPCO, PERCO, and CN3_SWF influenced soil characteristics and hydrological processes, including surface runoff, groundwater and evapotranspiration. Similarly, N'guessan et al. (2024) and Sánchez-Gómez et al. (2024) identified CN2, CN3_SWF, AWC, BD, and PERCO as sensitive to watershed evapotranspiration in the SWAT+ model.

4.2. Potential impacts of the ET spatial resolution, algorithms, and soil details on the accuracy of SWAT+ model simulations

RS data used as reference data for model calibration may be crucial for simulating key hydrological processes such as AET and improving their estimation (Lehmann et al., 2022). Our research work has introduced a stepwise calibration approach involving multisite data derived from multiple RS sources, which is essential for poorly gauged and ungauged catchments. This approach is unlike traditional methods, which generally use a single output parameter, namely discharge at the watershed outlet. Our comparison of the performances of SWAT+ models using different RS AET products revealed large variations in results depending on RS product, watershed and soil input data. This is in line with other studies (e.g. Bouizrou et al., 2023; Shah et al., 2021), which have indicated that the reliability of RS products varies according to region, climatic conditions and RS algorithms. Furthermore, our results showed that GLEAM outperformed MODIS in calibrating and validating all SWAT+ models, indicating that GLEAM is the most reliable AET product for the four watersheds of the Messinia region. In agreement with our findings, Dembélé et al. (2020), Ding and Zhu (2022), López López et al. (2017), Odusanya et al. (2019), and Taia et al. (2023) confirmed the reliability and superiority of GLEAM over MOD16A2 in Nigeria, West Africa, China, and Morocco, respectively.

The outperformance of GLEAM over MODIS can be attributed to the intrinsic characteristics of each remote sensing product. MODIS dependence on vapor pressure deficit results in increased model inaccuracies and higher uncertainties (Khan et al., 2018). Additionally, MOD16 does not incorporate soil moisture as an input variable, limiting its ability to capture irrigation effects in agricultural landscapes (Ding and Zhu, 2022; Tang et al., 2015; Xu et al., 2019). This is particularly relevant for the Messinia region, where the prevalent olive orchards are irrigated, while MOD16 tends to neglect the effect such practices, leading to higher model errors and uncertainties.

Furthermore, the poor AET performance of MODIS is partly explained by the small area of the four watersheds in the Messinia region (ranging from 25 to 90 km^2). The NASA Goddard's Global Modeling and Assimilation Office (GMAO) data used in MOD16 is primarily designed for macro-scale applications, making its accuracy questionable at finer spatial scales (Mu et al., 2011). At the micro-scale level of these watersheds, the inaccuracies in MOD16A2 become more evident (Mu et al., 2011). In small heterogeneous landscapes, MODIS faces challenges with land cover misclassification such as grasses, corn and trees often coexist within a single pixel (500 m resolution), affecting key biophysical parameters such as leaf area index (LAI) and albedo (Ruhoff et al., 2013). Such misclassification introduces further uncertainty in AET estimates (Ding and Zhu, 2022).

The relatively higher positive value of the PBIAS criterion obtained when validating the SWAT+ model particularly with MODIS indicates an underestimation of AET, a finding also reported by Jepsen et al. (2021), Koltsida and Kallioras (2020), Odusanya et al. (2019) and Weerasinghe et al. (2020). These studies noted that the dependence of MODIS on atmospheric moisture deficit leads to an underestimation of AET, especially during drought periods and under water stress conditions. Additionally, MOD16 higher relative uncertainty in croplands and irrigated areas (Souza et al., 2019) likely contributes to its underperformance in this study.

In comparison, GLEAM integrates a multi-layer soil moisture scheme and assimilates reliable satellite-based surface soil moisture data (Martens et al., 2017), allowing it to better capture water availability and irrigation effects. Moreover, GLEAM accounts for vegetation fraction and vegetation dynamics through remote sensing-based vegetation optical depth, which helps estimate crop water requirements more accurately than MOD16 (Huang et al., 2019). As a result, GLEAM exhibited the lowest PBIAS compared to the higher value by MOD16, namely during validation, further confirming its superior performance in representing AET in agricultural watersheds.

In terms of spatiotemporal resolution, GLEAM offers higher temporal but coarser spatial resolution. The coarser temporal resolution can affect ET accuracy and cause scaling mismatches in agrohydrological models. Nonetheless, several studies suggest that the impact of spatial resolution is often less significant than that of model parameters, model structure, and the quality of input data. For instance, Nkiaka et al. (2022) evaluated six satellite-based ET products across eight basins in Central-West Africa and showed the outperformance of GLEAM over products with a higher spatial resolution including MODIS. Similarly, Bennour et al. (2022) evaluated four remote sensing ET products including ETMonitor, GLEAM, SSEBop, and WaPOR using the SWAT model and both demonstrated and indicated that the SWAT model performance is not related to the spatial resolution of the evaluated ET products.

Messinia is a data-scarce region with limited soil information which makes it difficult to understand the hydrological processes in its four small-scale watersheds. Accordingly, this study assessed the accuracy of a novel high-resolution global soil product that provides a detailed soil data profile with six soil horizons. This product was compared to conventional, limited local soil data for micro-scale hydrological modeling using the SWAT+ model. Our results showed that the DSOLMap soil data performed slightly better than LOCSOL during calibration and somewhat improved performance during validation. While the MODIS AET simulations remained mostly unsatisfactory in terms of R^2 values, the use of DSOLMap did result in a slight improvement over LOCSOL. Although limited, this contributed to more accurate GLEAM and MODIS AET simulations when integrated with the SWAT+ model across the four watersheds. We attribute this outperformance to the DSOLMap database, which provides more soil classes and a more detailed profile with six layers, while LOCSOL has only one. A more detailed soil map better captures the physical processes in the SWAT+ model and improves AET simulation. Similar findings were reported by López-Ballesteros et al. (2023) who showed that DSOLMap significantly enhanced SWAT+ hydrological performance. Similarly, Wahren et al. (2016) compared the coarse-resolution FAO soil map (1:1000000) with two soil horizons to a more detailed map of effective soil depths, consisting of eight soil units, for the Águeda watershed. The detailed map developed using the SoLIM model, significantly improved SWAT model

simulations compared to the coarse-resolution FAO map. Overall, the detailed level of soil data input has an impact on the simulation of hydrological processes using hydrological models (Krpec et al., 2020; Rivas-Tabares et al., 2020).

4.3. Simulation of water balance components using SWAT+ model at watershed scale

The mean annual values of precipitation, evapotranspiration, and irrigation simulated by the SWAT+$_{\text{GLEAM\_DSOLMap}}$ model align with findings from Ekstedt (2013) in the Messinia region. Ekstedt (2013) computed the water balance for the Sellas, Gianouzagas, and Xerias watersheds from 2009 to 2012 using a simplified form of the water balance equation by assuming that inputs (precipitation) equal outputs (evapotranspiration and runoff), with any change in storage (ΔS) being negligible. Compared to our results, Ekstedt (2013) reported slightly lower evapotranspiration and irrigation values (484 mm < AET < 539 mm; 100 mm < irrigation < 150 mm), while precipitation values remain comparable (Table 7) (876 mm < precipitation < 916 mm) for each of the three watersheds. The ratio between AET and the water inputs, namely irrigation and precipitation, is similar in the Gianouzagas and Xerias watersheds, while it is higher for our model in the Sellas watershed. This is mainly due to the very high AET simulated in the Sellas watershed, which we attribute to the dominant forest land use, the highest percentage among the watersheds. Overall, the comparison of AET values with the percentage of forest land use in each watershed indicates a positive correlation: the higher the forest cover, the higher the AET (Tables 3,6). Furthermore, our irrigation values align with other Mediterranean studies in similar areas (e.g., Palomo et al., 2002; Tognetti et al., 2006), which estimated mean irrigation of olive orchards in southern Spain and southern Italy between 181 mm and 403 mm, respectively.

4.4. Effect of watershed characteristics on the SWAT+ performance

The Xerolagados watershed which has the highest percentage of agricultural land use reaching 89 %, was the only one of the four in the Messinia region where the SWAT+ model was not validated. This poor performance is likely due to complex evapotranspiration dynamics from agricultural land use and water bodies, particularly olives and the Gialova lagoon wetland (Maneas et al., 2019; Manzoni et al., 2020). More specifically, in this watershed, the unsatisfactory performances of MODIS are comparable with the other watersheds. Results instead strongly differed when using GLEAM, where we observed a remarkable reduction in AET peaks during the summer seasons (Fig. 9). Probably, irrigation in the prevalent olive orchard land use in the Xerolagados watershed was underestimated, leading to a consequent underestimation of AET. In this context, Dash et al. (2021) indicated that while SWAT is recognized for its capability in agro-hydrological modeling, its current ET al.gorithms do not adequately account for specific agricultural practices that influence ET rates, thus leading to potential inaccuracies in ET estimates. In addition, SWAT+ is sensitive to data inaccuracies in small watersheds. In addition, SWAT+ is sensitive to data inaccuracies in small watersheds. The Xerolagados watershed, the smallest in the Messinia region lacked a local meteorological station and relied on data from surrounding areas, which may have further contributed to the inaccuracies.

4.5. Implications for agro-hydrological Modeling in Mediterranean and Data-Scarce Regions

The main challenge for agro-hydrological modelers working in data-scarce regions is the limited availability of data, which prevents an accurate representation of hydrological and hydrodynamic processes with a high level of realism. This study's findings have significant implications for agro-hydrological modeling in Mediterranean and other data-scarce regions globally. Integrating freely available remote sensing AET, high-resolution global datasets, and SWAT+ management schedules has greatly improved the simulation of water cycle variables, particularly evapotranspiration.

The applicability of remotely sensed data for hydrological modeling has been demonstrated in various data-scarce regions beyond the Mediterranean. For instance, López López et al. (2017) successfully calibrated the PCR-GLOBWB model in the Oum Er-Rbia catchment in Morocco using GLEAM evapotranspiration and ESA CCI soil moisture, achieving reasonable discharge estimates. Similarly, studies in tropical regions, such as Nigeria where Odusanya et al. (2019) combined GLEAM AET data and the SWAT model to simulate AET in the watershed of the Ogun River Basin in Nigeria and showed the potential of GLEAM AET for calibrating and validating SWAT in data-scarce basins. In regions beyond the Mediterranean, Dile et al. (2020) employed remotely sensed AET to refine hydrological models in Ethiopia, highlighting its potential for assessing water management interventions aimed at environmental sustainability and agricultural productivity.

Our modeling approach can be replicated and scaled beyond data-scarce Mediterranean regions by fully leveraging remote sensing data products, such as AET, soil moisture for model calibration, and precipitation or air temperature data as model inputs at watershed, regional, and global scales. These datasets serve as alternatives to spatially and temporally limited data, enabling multivariate calibration and spatial calibration of hydrological models at the HRU and subbasin levels. This approach helps account for the spatial variability of hydrological processes, minimizes errors, and improves overall model accuracy. Additionally, soft calibration data (Moriasi et al., 2015b), such as ET ratios and mean annual runoff coefficients found in the literature, can further enhance the modeling process by providing additional constraints to improve model reliability in data-scarce regions.

4.6. Potential limitations of this approach

This study demonstrates that a comprehensive modeling approach, involving multisite calibration with high-resolution soil data, remote sensing data and detailed agricultural management practices as inputs to the SWAT+ model, improved the simulation results and accurately estimated the AET in the Messinia region. The initial comparison of AET estimates from GLEAM, MODIS, and FAO-56 P-M method, along with the use of multiple RS AET products combined with soil data in the multisite calibration approach, allowed us to identify the most accurate products, leading to reliable simulations of evapotranspiration. The lack of flow data has limited the ability to assess the accuracy of RS AET in estimating flow with the SWAT+ model. Using only AET data can produce a realistic representation of AET across the region but may not correctly represent the runoff component of the water balance. Despite this limitation, recent studies (e.g., Gleason and Durand, 2020; Jiang and Wang, 2019) have found that RS data can effectively predict hydrological variables, namely streamflow, in ungauged watersheds when combined with hydrological models. Similarly, López López et al. (2017) reported satisfactory flow simulation performance when the model was calibrated using GLEAM AET data alone. A multivariate calibration approach, such as using soil moisture and evapotranspiration data in the calibration and validation process, could further improve model simulations and provide a more realistic representation of water balance components at the watershed scale.

5. Conclusion

The integration of remote sensing data, high-resolution soil maps, and management schedules in the SWAT+ model provides valuable insights for improving water resource management in Messinia, a region with limited in-situ data. Our results demonstrate that GLEAM AET is the most suitable dataset for hydrological modeling in this region, as it closely matched the FAO-56 P-M method and significantly improved

model performance. Among the tested configurations, SWAT+-$_{\text{GLEAM\_DSOLMap}}$ emerged as the best-performing setup, achieving a mean NSE of 0.75 during calibration and 0.55 during validation with RSR values below 0.5 in most cases. In contrast, MODIS AET resulted in unsatisfactory performance, with high variation across watersheds and negative NSE values during validation, further confirming the superiority of GLEAM.

These findings have direct implications for agricultural water management in Messinia. Given the region's reliance on irrigated olive farming, our results highlight the importance of high-resolution soil data (DSOLMap) and accurate AET datasets (GLEAM) for improving irrigation scheduling and optimizing water use efficiency. Additionally, the multisite calibration approach enhanced the spatial consistency of the SWAT+ model, ensuring a more accurate representation of hydrological variability across heterogeneous landscapes. This approach enables site-specific irrigation strategies that can reduce water overexploitation and enhance drought resilience. Policymakers and practitioners can adopt this approach to develop tailored water management strategies based on local watershed characteristics.

Beyond Messinia, this RS-based SWAT+ modeling approach can be replicated in other Mediterranean and data-scarce regions worldwide. By integrating freely available remote sensing and high global datasets (e.g., GLEAM for AET, global soil maps, and climate variables), stakeholders can develop reliable hydrological simulations, supporting sustainable water resource management at watershed, regional and global scales.

Funding sources

This research was carried out within the SALAM-MED project funded under the Partnership for Research and Innovation in the Mediterranean Area (PRIMA) programme supported by the European Union. Grant Agreement number: [2123] [SALAM-MED] [Call 2021 Section 1 Water RIA].

CRediT authorship contribution statement

Elena Bresci: Writing – review & editing, Validation, Supervision, Funding acquisition. **Bouizrou Ismail:** Writing – original draft, Visualization, Software, Methodology, Investigation, Formal analysis. **Giulio Castelli:** Writing – review & editing, Validation, Supervision, Methodology, Conceptualization. **Gonzalo Anibal Cabrera:** Writing – original draft, Software. **Lorenzo Villani:** Writing – review & editing, Methodology. **Stavros Solomos:** Writing – review & editing. **Giorgos Maneas:** Writing – review & editing. **Christos Pantazis:** Writing – review & editing, Data curation.

Declaration of Competing Interest

The authors declare that they have no known competing financial interests or personal relationships that could have appeared to influence the work reported in this paper.

Acknowledgements

We acknowledge support from the University of Applied Sciences Weihenstephan-Triesdorf (HSWT) for Open Access publishing. We would also like to express our sincere appreciation to the European Union for their financial support of this research project. Profound appreciation is extended to the Messinia observatory, for providing access to the meteorological and local soil data used in this research.

Appendix A. Supporting information

Supplementary data associated with this article can be found in the online version at doi:10.1016/j.agwat.2025.109761.

Data availability

Data will be made available on request.

References

Abbaspour, K.C., Rouholahnejad, E., Vaghefi, S., Srinivasan, R., Yang, H., Klove, B., 2015. A continental-scale hydrology and water quality model for Europe: calibration and uncertainty of a high-resolution large-scale SWAT model. J. Hydrol. 524, 733–752. https://doi.org/10.1016/j.jhydrol.2015.03.027.

Abbaspour, K.C., Vaghefi, S.A.S., Yang, H., Srinivasan, R., 2019. Global soil, landuse, evapotranspiration, historical and future weather databases for SWAT applications. Sci. Data 6. https://doi.org/10.1038/s41597-019-0282-4.

Abiy, A.Z., Melesse, A.M., Seyoum, W.M., Abtew, W., 2019. Drought and climate teleconnection and drought monitoring. Extrem. Hydrol. Clim. Var. 275–295. https://doi.org/10.1016/B978-0-12-815998-9.00022-1.

Akoko, G., Le, T.H., Gomi, T., Kato, T., 2021. A review of SWAT model application in Africa. Water 13, 1313. https://doi.org/10.3390/w13091313.

Allen, R.G., Pereira, L.S., Raes, D., Smith, M., 1998. Crop evapotranspiration-Guidelines for computing crop water requirements-FAO irrigation and drainage paper 56. Fao Rome 300 (9), D05109. ⟨https://www.fao.org/4/x0490e/x0490e00.htm⟩.

Amin, A., Iqbal, J., Asghar, A., Ribbe, L., 2018. Analysis of current and future water demands in the upper Indus basin under IPCC climate and socio-economic scenarios using a hydro-economic WEAP model. Water 10 (5), 537. https://doi.org/10.3390/w10050537.

Aqnouy, M., Ahmed, M., Ayele, G.T., Bouizrou, I., Bouadila, A., Stitou El Messari, J.E., 2023. Comparison of hydrological platforms in assessing rainfall-runoff behavior in a Mediterranean watershed of Northern Morocco. Water 15 (3), 447. https://doi.org/10.3390/w15030447.

Arnold, J.G., Bieger, K., White, M.J., Srinivasan, R., Dunbar, J.A., Allen, P.M., 2018. Use of decision tables to simulate management in SWAT. Water 10, 713. https://doi.org/10.3390/w10060713.

Arnold, J.G., Moriasi, D.N., Gassman, P.W., Abbaspour, K.C., White, M.J., Srinivasan, R., Santhi, C., Harmel, R.D., van Griensven, A., Van Liew, M.W., Kannan, N., Jha, M.K., 2012. Swat: model use, calibration, and validation. Trans. ASABE 55, 1491–1508. https://doi.org/10.13031/2013.42256.

Arnold, J.G., Srinivasan, R., Muttiah, R.S., Williams, J.R., 1998. Large area hydrologic modeling and assesment part I: model development. JAWRA J. Am. Water Resour. Assoc. 34, 73–89. https://doi.org/10.1111/j.17521688.1998.tb05961.x,1998.

Asfaw, A., Simane, B., Hassen, A., Bantider, A., 2018. Variability and time series trend analysis of rainfall and temperature in northcentral Ethiopia: a case study in woleka sub-basin. Weather Clim. Extrem 19, 29–41. https://doi.org/10.1016/j.wace.2017.12.002,2018.

Bañares, E.N., Mehboob, M.S., Khan, A.R., Cacal, J.C., 2024. Projecting hydrological response to climate change and urbanization using WEAP model: a case study for the main watersheds of bicol river basin, Philippines. J. Hydrol. Reg. Stud. 54, 101846. https://doi.org/10.1016/j.ejrh.2024.101846.

Basu, A.S., Gill, L.W., Pilla, F., Basu, B., 2022. Assessment of variations in runoff due to landcover changes using the SWAT model in an urban river in Dublin, Ireland. Sustainability 14 (1), 534. https://doi.org/10.3390/su14010534.

Bennour, A., Jia, L., Menenti, M., Zheng, C., Zeng, Y., Asenso Barnieh, B., Jiang, M., 2022. Calibration and validation of SWAT model by using hydrological remote sensing observables in the lake Chad basin. Remote Sens. 14 (6), 1511. https://doi.org/10.3390/rs14061511.

Berg, H., Maneas, G., Salguero Engström, A., 2018. A comparison between organic and conventional olive farming in messenia, Greece. Horticulturae 4 (3), 15. https://doi.org/10.3390/horticulturae4030015.

Bieger, K., Arnold, J.G., Rathjens, H., White, M.J., Bosch, D.D., Allen, P.M., Volk, M., Srinivasan, R., 2017. Introduction to SWAT plus, a completely restructured version of the soil and water assessment tool. J. Am. Water Resour. Assoc. 53, 115–130. https://doi.org/10.1111/1752-1688.12482.

Bieger, K., Arnold, J.G., Rathjens, H., White, M.J., Bosch, D.D., Allen, P.M., 2019. Representing the connectivity of upland areas to floodplains and streams in SWAT. J. Am. Water Resour. Assoc. 55, 578–590. https://doi.org/10.1111/1752-1688.12728.

Bouizrou, I., Aqnouy, M., Bouadila, A., En-Nagre, K., Hilal, I., Mliyeh, M.M., Benaabidate, L., 2025. Modeling approaches to enhance the accuracy of streamflow and hydrological signature simulations in data-scarce Mediterranean regions: insights from oued issen, Morocco. Mediterr. Geosci. Rev. 1–16. https://doi.org/10.1007/s42990-025-00159-5.

Bouizrou, I., Bouadila, A., Aqnouy, M., Gourfi, A., 2023. Assessment of remotely sensed precipitation products for climatic and hydrological studies in arid to semi-arid data-scarce region, central-Western Morocco. Remote Sens. Appl. Soc. Environ. 30, 100976. https://doi.org/10.1016/j.rsase.2023.100976.

Bouizrou, I., Chahinian, N., Perrin, J.L., Müller, R., Rais, N., 2021. Network representation in hydrological modelling on urban catchments in data-scarce contexts: a case study on the oued fez catchment (Morocco). J. Hydrol. Reg. Stud. 34, 100800. https://doi.org/10.1016/j.ejrh.2021.100800.

Bronstert, A., Plate, E.J., 1997. Modelling of runoff generation and soil moisture dynamics for hillslopes and micro-catchments. J. Hydrol. 198 (1-4), 177–195. https://doi.org/10.1016/S0022-1694(96)03306-9.

Centeno, L.N., Hu, W., Timm, L.C., She, D., da Silva Ferreira, A., Barros, W.S., Caldeira, T.L., 2020. Dominant control of macroporosity on saturated soil hydraulic

conductivity at multiple scales and locations revealed by wavelet analyses. J. Soil Sci. Plant Nutr. 20 (4), 1686–1702. https://doi.org/10.1007/s42729-020-00239-5.
Chun, J.A., Baik, J., Kim, D., Choi, M., 2018. A comparative assessment of SWAT-model-based evapotranspiration against regional-scale estimates. Ecol. Eng. 122, 1–9. https://doi.org/10.1016/j.ecoleng.2018.07.015.
Clark, M.P., Fan, Y., Lawrence, D.M., Adam, J.C., Bolster, D., Gochis, D.J., Zeng, X., 2015. Improving the representation of hydrologic processes in earth system models. Water Resour. Res. 51 (8), 5929–5956. https://doi.org/10.1002/2015WR017096.
Dai, Y.J., Wei, S.G., Nan, W., Xin, Q.C., Hua, Y., Zhang, S.P., Liu, S.F., Lu, X.J., Wang, D. G., Yan, F.P., 2019. A review of the global soil property maps for earth system models. SoilGer. 5 (2), 137–158. https://doi.org/10.5194/soil-5-137-2019.
Dash, S.S., Sahoo, B., Raghuwanshi, N.S., 2021. How reliable are the evapotranspiration estimates by soil and water assessment tool (SWAT) and variable infiltration capacity (VIC) models for catchment-scale drought assessment and irrigation planning? J. Hydrol. 592, 125838. https://doi.org/10.1016/j.jhydrol.2020.125838.
Dembélé, M., Ceperley, N., Zwart, S.J., Salvadore, E., Mariethoz, G., Schaefli, B., 2020. Potential of satellite and reanalysis evaporation datasets for hydrological modelling under various model calibration strategies. Adv. Water Resour. 143, 103667. https://doi.org/10.1016/j.advwatres.2020.103667.
Desertification Research Center, University of Sassari. (2021). SALAM-MED – Sustainable Approaches to Land and Water Management in Mediterranean Drylands. Funded under the PRIMA 2021 Programme, Section 1. Retrieved from https://www.salam-med.org/.
Dile, Y.T., Ayana, E.K., Worqlul, A.W., Xie, H., Srinivasan, R., Lefore, N., Clarke, N., 2020. Evaluating satellite-based evapotranspiration estimates for hydrological applications in data-scarce regions: a case in Ethiopia. Sci. Total Environ. 743, 140702. https://doi.org/10.1016/j.scitotenv.2020.140702.
Ding, J., Zhu, Q., 2022. The accuracy of multisource evapotranspiration products and their applicability in streamflow simulation over a large catchment of Southern China. J. Hydrol. Reg. Stud. 41, 101092. https://doi.org/10.1016/j.ejrh.2022.101092.
Dou, X., Shi, H., Li, R., Miao, Q., Yan, J., Tian, F., Wang, B., 2022. Simulation and evaluation of soil water and salt transport under controlled subsurface drainage using HYDRUS-2D model. Agric. Water Manag. 273, 107899. https://doi.org/10.1016/j.agwat.2022.107899.
Eini, M.R., Salmani, H., Piniewski, M., 2023. Comparison of process-based and statistical approaches for simulation and projections of rainfed crop yields. Agric. Water Manag 277, 108107. https://doi.org/10.1016/j.agwat.2022.108107.
Ekstedt, K., 2013. Local water resource assessment in messinia, Greece. Master D. Thesis. University of Stockholm, pp. 1–55. ⟨https://www.diva-portal.org/smash/get/diva2:643960/FULLTEXT01.pdf⟩.
Essenfelder, A.H., 2016. SWAT Weather Database: A Quick Guide. Version: v.0.16.07. doi:10.13140/RG.2.1.4329.1927.
European Environment Agency, 2021. CORINE Land Cover 2018 (Version 20.5). Copernicus Land Monitoring Service. ⟨https://land.copernicus.eu/pan-european/corine-land-cover⟩.
Falamarzia, Y., Palizdana, N., Feng Huang, Y., ShuiLee, T., 2014. Estimating evapotranspiration from temperature and wind speed data using artificial and wavelet neural networks (WNNs). Agric. Water Manag. 140, 26–36. https://doi.org/10.1016/j.agwat.2014.03.014.
FAO, 2003. Digital soil map of the world and derived soil properties (Version 3.6). Food and Agriculture Organization of the United Nations. https://www.fao.org/soils-portal/soil-survey/soil-maps-and-databases/digital-soil-map-of-the-world/en/.
FAO/IIASA/ISRIC/ISS-CAS/JRC, 2012. Harmonized world soil database (version 1.2). FAO, Rome, Italy and IIASA, Laxenburg, Austria. ⟨https://www.fao.org/soils-portal/soil-survey/soil-maps-and-databases/harmonized-world-soil-database-v12/ru/⟩.
FAO-UNESCO, 2003a. The Digital Soil Map of the World, Version 3.6, Land and Water Development Division, Rome, Italy. ⟨https://www.fao.org/land-water/land/land-governance/land-resources-planning-toolbox/category/details/en/c/1026564/⟩.
Faramarzi, M., Abbaspour, K.C., Lu, W., Fennell, J., Zehnder, A.J., Goss, G.G., 2017. Uncertainty based assessment of dynamic freshwater scarcity in semi-arid watersheds of alberta, Canada. J. Hydrol. Reg. Stud. 9, 48–68. https://doi.org/10.1016/j.ejrh.2016.11.003.
Fatichi, S., Vivoni, E.R., Ogden, F.L., Ivanov, V.Y., Mirus, B., Gochis, D., Tarboton, D., 2016. An overview of current applications, challenges, and future trends in distributed process-based models in hydrology. J. Hydrol. 537, 45–60. https://doi.org/10.1016/j.jhydrol.2016.03.026.
Ferreira, R.G., Dias, R.L.S., de Siqueira Castro, J., dos Santos, V.J., Calijuri, M.L., da Silva, D.D., 2021. Performance of hydrological models in fluvial flow simulation. Ecol. Inform. 66, 101453. https://doi.org/10.1016/j.ecoinf.2021.101453.
Food and Agriculture Organization (FAO), 1998. Crop evapotranspiration – Guidelines for computing crop water requirements (FAO Irrigation and Drainage Paper No. 56). Food and Agriculture Organization of the United Nations. ⟨https://www.fao.org/3/x0490e/x0490e00.html⟩.
Fu, B., Merritt, W.S., Croke, B.F., Weber, T.R., Jakeman, A.J., 2019. A review of catchment-scale water quality and erosion models and a synthesis of future prospects. Environ. Model. Softw. 114, 75–97. https://doi.org/10.1016/j.envsoft.2018.12.008.
Gitau, M.W., Chaubey, I., 2010. Regionalization of SWAT model parameters for use in ungauged watersheds. Water 2 (4), 849–871. https://doi.org/10.3390/w2040849.
Gleason, C.J., Durand, M.T., 2020. Remote sensing of river discharge: a review and a framing for the discipline. Remote Sens 12, 1107. https://doi.org/10.3390/rs12071107.
Govindaraju, R.S., Kavvas, M.L., Jones, S.E., Rolston, D.E., 1996. Use of Green-Ampt model for analyzing one-dimensional convective transport in unsaturated soils. J. Hydrol. 178 (1-4), 337–350. https://doi.org/10.1016/0022-1694(95)02796-3.
Hargreaves, G.H., Samani, Z.A., 1985. Reference crop evapotranspi- ration from temperature, 1985 Appl. Engr. Agric. 1, 96–99. https://doi.org/10.13031/2013.26773.
Hengl, T., MacMillan, R. A., 2019. Statistical theory for predictive soil mapping [Chapter]. In Predictive Soil Mapping with R. OpenGeoHub Foundation. Retrieved from https://soilmapper.org/statistical-theory.html.
Himanshu, S.K., Pandey, A., Karki, K., Pandey, R.P., Palmate, S.S., Datta, A., 2023. Assessing the applicability of variable infiltration capacity (VIC) model using remote sensing products for the analysis of water balance: case study of the tons river basin, India. J. Indian Soc. Remote Sens. 51 (11), 2323–2341. https://doi.org/10.1007/s12524-023-01768-z.
Huang, S., Eisner, S., Haddeland, I., Mengistu, Z.T., 2022. Evaluation of two new-generation global soil databases for macro-scale hydrological modelling in Norway. J. Hydrol. 610, 127895. https://doi.org/10.1016/j.jhydrol.2022.127895.
Huang, J., Gómez-Dans, J.L., Huang, H., Ma, H., Wu, Q., Lewis, P.E., Xie, X., 2019. Assimilation of remote sensing into crop growth models: current status and perspectives. Agric. For. Meteorol. 276, 107609. https://doi.org/10.1016/j.agrformet.2019.06.008.
IPCC, 2021. In: V. Masson-Delmotte, P. Zhai, A. Pirani, S. L. Connors, C. Péan, S. Berger, N. Caud, Y. Chen, L. Goldfarb, M. I. Gomis, M. Huang, K. Leitzell, E. Lonnoy, J. B. R. Matthews, T. K. Maycock, T. Waterfield, O. Yelekçi, R. Yu, Zhou B., 2021. Climate change 2021: The physical science basis. Contribution of Working Group I to the Sixth Assessment Report of the Intergovernmental Panel on Climate Change. Cambridge University Press. https://doi.org/10.1017/9781009157896.
ISRIC, ISS-CAS, FAO. Harmonized World Soil Database (Version 1.2). Food and Agriculture Organization of the United Nations (FAO) and International Institute for Applied Systems Analysis (IIASA). https://www.fao.org/soils-portal/soil-survey/soil-maps-and-databases/harmonized-world-soil-database-v12/ru/.
Jepsen, S.M., Harmon, T.C., Guan, B., 2021. Analyzing the suitability of remotely sensed ET for calibrating a watershed model of a Mediterranean montane forest. Remote Sens. 13 (7), 1258. https://doi.org/10.3390/rs13071258.
Jiang, D., Wang, K., 2019. The role of satellite-based remote sensing in improving simulated streamflow: a review. Water (Basel) 11, 1615. https://doi.org/10.3390/w11081615.
Jiménez-Navarro, I.C., Pierson, D., Senent-Aparicio, J., 2024. The implications of the use of ET remote sensing data for calibrating hydrological models: a comparison of single and Multi-criteria calibration in SWAT+. Earth Syst. Environ. 1–17. https://doi.org/10.1007/s41748-024-00438-5.
Kadam, S.A., Gorantiwar, S.D., Mandre, N.P., Tale, D.P., 2021. Crop coefficient for potato crop evapotranspiration estimation by field water balance method in semi-arid region, maharashtra, India. Potato Res 64 (3), 421–433. https://doi.org/10.1007/s11540-020-09484-8.
Kakkavou, K., Gemtou, M., Fountas, S., 2024. Drivers and barriers to the adoption of precision irrigation technologies in olive and cotton farming—Lessons from messenia and thessaly regions in Greece. Smart Agric. Technol. 7, 100401. https://doi.org/10.1016/j.atech.2024.100401.
Kalabokidis, K., Palaiologou, P., Gerasopoulos, E., Giannakopoulos, C., Kostopoulou, E., Zerefos, C., 2015. Effect of climate change projections on forest fire behavior and values-at-risk in southwestern Greece. Forests 6 (6), 2214–2240. https://doi.org/10.3390/f6062214.
Kardhana, H., Lihawa, A.W.I., Rohmat, F.I.W., Wulandari, S., Harjupa, W., Adiprawita, W., Kusuma, M.S.B., 2024. Water balance analysis in the majalaya watershed: Two-Step calibration and application of the SWAT+ model for Low-Flow conditions. Water 16 (23), 3498. https://doi.org/10.3390/w16233498.
Khan, N.M., Negi, A., Thaseen, I.S., 2018. Analysis on improving the performance ofmachine learning models using feature selection technique. international conference on intelligent systems design and applications. Springer. https://doi.org/10.1007/978-3-030-16660-1_7.
Klein, J., Ekstedt, K., Walter, M.T., Lyon, S.W., 2015. Modeling potential water resource impacts of Mediterranean tourism in a changing climate. Environ. Model. Assess. 20, 117–128. https://doi.org/10.1007/s10666-014-9418-2.
Klemeš, V., 1986. Operational testing of hydrological simulation models. Hydrol. Sci. 3 (1–3), 13–24. https://doi.org/10.1080/02626668609491024.
Kofidou, M., Gemitzi, A., 2023. Assimilating soil moisture information to improve the performance of swat hydrological model. Hydrology 10 (8), 176. https://doi.org/10.3390/hydrology10080176.
Koltsida, E., Kallioras, A., 2022. Multi-variable SWAT model calibration using satellitebased evapotranspiration data and streamflow. Hydrology 9, 112. https://doi.org/10.3390/hydrology9070112.
Krpec, P., Horáček, M., Šarapatka, B., 2020. A comparison of the use of local legacy soil data and global datasets for hydrological modelling a small-scale watershed: implications for nitrate loading estimation. Geoderma 377 (February). https://doi.org/10.1016/j.geoderma.2020.114575.
Lankford, B.A., 2023. Resolving the paradoxes of irrigation efficiency: irrigated systems accounting analyses depletion-based water conservation for reallocation. Agric. Water Manag. 287, 108437. https://doi.org/10.1016/j.agwat.2023.108437.
Lehmann, F., Vishwakarma, B.D., Bamber, J., 2022. How well are we able to close the water budget at the global scale? Hydrol. Earth Syst. Sci. 26 (1), 35–54. https://doi.org/10.5194/hess-26-35-2022.
Lenhart, T., Eckhardt, K., Fohrer, N., Frede, H.G., 2002. Comparison of two different approaches of sensitivity analysis. Phys. Chem. Earth 27, 645–654. https://doi.org/10.1016/S1474-7065(02)00049-9.
Levidow, L., Zaccaria, D., Maia, R., Vivas, E., Todorovic, M., Scardigno, A., 2014. Improving water-efficient irrigation: prospects and difficulties of innovative practices. Agric. Water Manag. 146, 84–94. https://doi.org/10.1016/j.agwat.2014.07.012.

Liang, X., Lettenmaier, D.P., Wood, E.F., Burges, S.J., 1994. A simple hydrologically based model of land surface water and energy fluxes for general circulation models. J. Geophys Res. https://doi.org/10.1029/94JD00483.
Licciardello, F., Rossi, C.G., Srinivasan, R., Zimbone, S.M., Barbagallo, S., 2011. Hydrologic evaluation of a Mediterranean watershed using the SWAT model with multiple PET estimation methods. Trans. ASABE 54, 1615–1625 http://ssl.tamu.edu/media/49873/feliciana-etpaper.pdf.
Liu, S., Xu, Z., Song, L., Zhao, Q., Ge, Y., Xu, T., Zhang, F., 2016. Upscaling evapotranspiration measurements from multi-site to the satellite pixel scale over heterogeneous land surfaces. Agric. For. Meteorol. 230, 97–113. https://doi.org/10.1016/j.agrformet.2016.04.008.
López López, P., Sutanudjaja, E.H., Schellekens, J., Sterk, G., Bierkens, M.F., 2017. Calibration of a large-scale hydrological model using satellite-based soil moisture and evapotranspiration products. Hydrol. Earth Syst. Sci. 21 (6), 3125–3144. https://doi.org/10.5194/hess-21-3125-2017,2017.
López-Ballesteros, A., Nielsen, A., Castellanos-Osorio, G., Trolle, D., Senent-Aparicio, J., 2023. DSOLMap, a novel high-resolution global digital soil property map for the SWAT+ model: development and hydrological evaluation. Catena 231, 107339. https://doi.org/10.1016/j.catena.2023.107339.
López-Ballesteros, A., Senent-Aparicio, J., Srinivasan, R., Pérez-Sánchez, J., 2019. Assessing the impact of best management practices in a highly anthropogenic and ungauged watershed using the SWAT model: a case study in the el beal watershed (Southeast Spain). Agronomy 9 (10), 1–15. https://doi.org/10.3390/agronomy9100576.
López-Ramírez, S.M., Mayer, A., Sáenz, L., Muñoz-Villers, L.E., Holwerda, F., Looker, N., Schürz, C., Berry, Z.C., Manson, R., Asbjornsen, H., Kolka, R., Geissert, D., Lezama, C., 2021. A comprehensive calibration and validation of SWAT-T using local datasets, evapotranspiration and streamflow in a tropical montane cloud forest area with permeable substrate in central veracruz, Mexico. J. Hydrol. 603 (July). https://doi.org/10.1016/j.jhydrol.2021.126781.
Loukas, A., Vasiliades, L., Domenikiotis, C., Dalezios, N.R., 2005. Basin-wide actual evapotranspiration estimation using NOAA/AVHRR satellite data. Phys. Chem. Earth Parts A/B/C. 30 (1–3), 69–79. https://doi.org/10.1016/j.pce.2004.08.023.
Lu, Z., Wei, Y., Feng, Q., Western, A.W., Zhou, S., 2018. A framework for incorporating social processes in hydrological models. Curr. Opin. Environ. Sustain. 33, 42–50. https://doi.org/10.1016/j.cosust.2018.04.011.
Maneas, G., Makopoulou, E., Bousbouras, D., Berg, H., Manzoni, S., 2019. Anthropogenic changes in a Mediterranean coastal wetland during the last century. The case of gialova lagoon, messinia, Greece. Water 11 (2), 350. https://doi.org/10.3390/w11020350.
Manzoni, S., Maneas, G., Scaini, A., Psiloglou, B.E., Destouni, G., Lyon, S.W., 2020. Understanding coastal wetland conditions and futures by closing their hydrologic balance: the case of the gialova lagoon, Greece. Hydrol. Earth Syst. Sci. 24 (7), 3557–3571. https://doi.org/10.5194/hess-24-3557-2020.
Martens, B., Miralles, D.G., Lievens, H., Van Der Schalie, R., De Jeu, R.A., Fernández-Prieto, D., Verhoest, N.E., 2017. GLEAM v3: Satellite-based land evaporation and root-zone soil moisture. Geosci. Model Dev. 10 (5), 1903–1925. https://doi.org/10.5194/gmd-10-1903-2017.
MedECC, 2020. Climate and Environmental Change in the Mediterranean Basin – Current Situation and Risks for the Future. First Mediterranean Assessment Report [Cramer, W., Guiot, J., Marini, K., 2020.Union for the Mediterranean, Plan Bleu, UNEP/MAP, Marseille, France, 632pp, ISBN 978-2-9577416-0-1, doi: 10.5281/zenodo.4768833.
Mehboob, M.S., Kim, Y., 2021. Effect of climate and socioeconomic changes on future surface water availability from mountainous water sources in Pakistan's Upper Indus Basin. Sci. Total Environ. 769, 144820. https://doi.org/10.1016/j.scitotenv.2020.144820.
Merz, J., Mosley, M.P., 1998. Hydrological behaviour of pastoral hill country modified by extensive landsliding, Northern hawke's bay, New Zealand. J. Hydrol. (N. Z.) 113–139. ⟨https://www.scopus.com/record/display.uri?eid=2-s2.0-0005652295&origin=inward&txGid=48dfcd097b93b53bd531b1e6694dfa4c⟩.
Michaud, J., Sorooshian, S., 1994. Comparison of simple versus complex distributed runoff models on a midsized semiarid watershed. Water Resour. Res. 30 (3), 593–605. https://doi.org/10.1029/93WR03218.
Miralles, D.G., Holmes, T.R.H., de Jeu, R.A.M., Gash, J.H., Meesters, A.G.C.A., Dolman, A.J., 2011. Global land-surface evaporation estimated from satellite-based observations. Hydrol. Earth Syst. Sci. 15, 453–469. https://doi.org/10.5194/hess-15-453-2011.
Mohammadi, B., Moazenzadeh, R., Christian, K., Duan, Z., 2021. Improving streamflow simulation by combining hydrological process-driven and artificial intelligence-based models. Environ. Sci. Pollut. Res. 28 (46), 65752–65768. https://doi.org/10.1016/j.jhydrol.2019.123981.
Monteith, J.L., 1965. Evaporation and environment. Symp. Soc. Exp. Biol. 19, 205–234.
Monteith J, L, 1965. Evaporation and the environment. In the state and movement of water in living organisms. XIXth Symposium. Soc. for Exp. Biol. Cambridge University Press, Swansea, pp. 205–234. ⟨https://repository.rothamsted.ac.uk/item/8v5v7/evaporation-and-environment⟩.
Moore, I.D., Gessler, P.E., Nielsen, G.A.E., Peterson, G.A., 1993. Soil attribute prediction using terrain analysis. Soil Sci. Soc. Am. J. 57 (2), 443–452. https://doi.org/10.2136/sssaj1993.03615995005700020026x.
Moriasi, D.N., Arnold, J.G., Van Liew, M.W., Bingner, R.L., Harmel, R.D., Veith, T.L., 2007. Model evaluation guidelines for systematic quantification of accuracy in watershed simulations. Trans. ASABE 50, 885–900. https://doi.org/10.5194/hessd-7-8479-2010.
Moriasi, D.N., Gitau, M.W., Pai, N., Daggupati, P., 2015b. Hydrologic and water quality models: performance measures and evaluation criteria. Trans. ASABE 58 (6), 1763–1785 doi: 0.13031/trans.58.10715.
Moriasi, D.N., Zeckoski, R.W., Arnold, J.G., Baffaut, C., Malone, R.W., Daggupati, P., Douglas-Mankin, K.R., 2015a. Hydrologic and water quality models: key calibration and validation topics. Trans. ASABE 58 (6), 1609–1618. https://doi.org/10.13031/trans.58.11075.
Mu, Q., Zhao, M., Running, S.W., 2011. Improvements to a MODIS global terrestrial evapotranspiration algorithm. Remote Sens. Environ. 115 (8), 1781–1800. https://doi.org/10.1016/j.rse.2011.02.019.
Mu, Q., Zhao, M., Running, S.W., 2013. MODIS global terrestrial evapotranspiration (ET) product (NASA MOD16A2/A3). Algorithm Theor. Basis Doc. Collect. 5 (600), 381–394. ⟨https://modis-land.gsfc.nasa.gov/pdf/MOD16ATBD.pdf⟩.
Neitsch, S.L., Arnold, J.G., Kiniry, J.R., Williams, J.R., and King, K.W., 2002. Soil and water assessment tool theoretical documentation, Texas Water Resour. Inst., 494, available at: ⟨http://www.scopus.com/inward/record.url?eid=2-s2.0-0011239709&partnerID=tZOtx3y1⟩ (last access: 11 January 2017), 2002.
Neitsch, S.L., Arnold, J.G., Kiniry, J.R., and Williams, J.R., 2005. Soil and Water Assessment Tool (SWAT) Theoretical Documentation. Blackland Research Center, Texas Agricultural Experiment Station and Grassland, Soil and Water Research Laboratory, Temple, TX, 2005. ⟨https://swat.tamu.edu/media/99192/swat2009-theory.pdf⟩.
Neitsch, S. L., Arnold, J. G., Kiniry, J. R., Williams, J. R., 2011. Soil and Water Assessment Tool: Theoretical Documentation Version 2009 (Technical Report No. 406). Texas Water Resources Institute, Texas A&M University.
N'guessan, J.Y.K., Adahi, B.M., Konan-Waidhet, A.B., Kra, J.L., Koffi, B., Habel, M., Assidjo, E.N., 2024. Using the SWAT+ model to assess the conditions of water inflow to a reservoir in an uncontrolled agricultural catchment. Case Study Nanan Reserv. Lake Taabo Catchment (C. ôte D. 'Ivoire). Ecohydrol. Hydrobiol. 24 (3), 568–582. https://doi.org/10.1016/j.ecohyd.2023.08.002.
Nkiaka, E., Bryant, R.G., Ntajal, J., Biao, E.I., 2022. Evaluating the accuracy of gridded water resources reanalysis and evapotranspiration products for assessing water security in poorly gauged basins. Hydrol. Earth Syst. Sci. 26 (22), 5899–5916. https://doi.org/10.5194/hess-26-5899-2022.
Nourani, V., Tootoonchi, R., Andaryani, S., 2021. Investigation of climate, land cover and lake level pattern changes and interactions using remotely sensed data and wavelet analysis. Ecol. Inform. 64, 101330. https://doi.org/10.1016/j.ecoinf.2021.101330.
Odusanya, A.E., Mehdi, B., Schürz, C., Oke, A.O., Awokola, O.S., Awomeso, J.A., Schulz, K., 2019. Multi-site calibration and validation of SWAT with satellite-based evapotranspiration in a data-sparse catchment in southwestern Nigeria. Hydrol. Earth Syst. Sci. 23 (2), 1113–1144. https://doi.org/10.5194/hess-23-1113-2019.
OpenDEM. 2023. OpenDEM: Digital Elevation Models from ALOS PALSAR and SRTM. ⟨https://www.opendem.info/about.html⟩.
Palomo, M.J., Moreno, F., Fernández, J.E., Díaz-Espejo, A., Girón, I.F., 2002. Determining water consumption in olive orchards using the water balance approach. Agric. Water Manag. 55 (1), 15–35. https://doi.org/10.1016/S0378-3774(01)00182-2.
Paniconi, C., Putti, M., 2015. Physically based modeling in catchment hydrology at 50: survey and outlook. Water Resour. Res. 51 (9), 7090–7129. https://doi.org/10.1002/2015WR017780.
Parajuli, P.B., Jayakody, P., Ouyang, Y., 2018. Evaluation of using remote sensing evapotranspiration data in SWAT. Water Resour. Manag. 32, 985–996. https://doi.org/10.1007/s11269-017-1850-z.
Penman, H.L., 1956. Evaporation: an introductory survey. Neth. J. Agric. Sci. Reboita. https://doi.org/10.18174/njas.v4i1.17768.
Priestley, C., Taylor, R., 1972. On the assessment of surface heat flux and evaporation using large-scale parameters, 1972 Mon. Weather Rev. 100, 81–92. https://doi.org/10.1175/1520-0493(1972)100%3C0081:OTAOSH%3E2.3.CO;2.
Pulighe, G., Lupia, F., Chen, H., Yin, H., 2021. Modeling climate change impacts on water balance of a Mediterranean watershed using SWAT+. Hydrology 8 (4), 157. https://doi.org/10.3390/hydrology8040157.
Qiao, L., Will, R., Wagner, K., Zhang, T., Zou, C., 2022. Improvement of evapotranspiration estimates for grasslands in the Southern great plains: comparing a biophysical model (SWAT) and remote sensing (MODIS). J. Hydrol. Reg. Stud. 44, 101275. https://doi.org/10.1016/j.ejrh.2022.101275.
Rajib, A., Evenson, G.R., Golden, H.E., Lane, C.R., 2018. Hydrologic model predictability improves with spatially explicit calibration using remotely sensed evapotranspiration and biophysical parameters. J. Hydrol. 567, 668–683. https://doi.org/10.1016/j.jhydrol.2018.10.024.
Razavi, S., 2021. Deep learning, explained: fundamentals, explainability, and bridgeability to process-based modelling. Environ. Model Ling. Softw. 144, 105159. https://doi.org/10.1016/j.envsoft.2021.105159.
Rientjes, T.H.M., Muthuwatta, L.P., Bos, M.G., Booij, M.J., Bhatti, H.A., 2013. Multivariable calibration of a semi-distributed hydrological model using streamflow data and satellite-based evapotranspiration. J. Hydrol. 505, 276–290. https://doi.org/10.1016/j.jhydrol.2013.10.006.
Rivas-Tabares, D., de Miguel, Á., Willaarts, B., Tarquis, A.M., 2020. Self-organizing map of soil properties in the context of hydrological modeling. Appl. Math. Model. 88, 175–189. https://doi.org/10.1016/j.apm.2020.06.044.
Roy, T., Gupta, H.V., Serrat-Capdevila, A., Valdes, J.B., 2017. Using satellite-based evapotranspiration estimates to improve the structure of a simple conceptual rainfall–runoff model. Hydrol. Earth Syst. Sci. 21 (2), 879–896. https://doi.org/10.5194/hess-21-879-2017.
Ruhoff, A.L., Paz, A.R.D., Aragao, L.E., Mu, Q., Malhi, Y., Collischonn, W., Running, S.W., 2013. Assessment of the MODIS global evapotranspiration algorithm using eddy covariance measurements and hydrological modelling in the Rio Grande basin. Hydrol. Sci. J. 58 (8), 1658–1676. https://doi.org/10.1080/02626667.2013.837578.

Running, S., Mu, Q., Zhao, M., 2017. MOD16A2 MODIS/Terra Net Evapotranspiration 8-Day L4 Global 500m SIN Grid V006 [Data set]. NASA EOSDIS Land Processes Distributed Active Archive Center. Accessed 2024-08-10 from https://doi.org/10.5067/MODIS/MOD16A2.006.

Running, S., Mu, Q., Zhao, M., 2021. MODIS/Terra Net Evapotranspiration 8-Day L4 Global 500m SIN Grid V061 [Data set]. NASA EOSDIS Land Processes Distributed Active Archive Center. Accessed 2024-10-14 from https://doi.org/10.5067/MODIS/MOD16A2.061.

Running, S.W., Mu, Q., Zhao, M., Moreno, A., 2019. MODIS global terrestrial evapotranspiration (ET) product (MOD16A2/A3 and year-end gap-filled MOD16A2GF/A3GF) NASA Earth Observing System MODIS Land Algorithm (for collection 6). National Aeronautics and Space Administration, Washington, DC, USA, https://doi.org/10.5067/MODIS/MOD16A2,6.

Sánchez-Gómez, A., Schürz, C., Molina-Navarro, E., Bieger, K., 2024. Groundwater modelling in SWAT+: considerations for a realistic baseflow simulation. Groundw. Sustain. Dev. 26, 101275. https://doi.org/10.1016/j.gsd.2024.101275.

Sertel, E., Imamoglu, M.Z., Cuceloglu, G., Erturk, A., 2019. Impacts of land cover/use changes on hydrological processes in a rapidly urbanizing mid-latitude water supply catchment. Water 11 (5), 1075. https://doi.org/10.3390/w11051075.

Shah, S., Duan, Z., Song, X., Li, R., Mao, H., Liu, J., Wang, M., 2021. Evaluating the added value of multi-variable calibration of SWAT with remotely sensed evapotranspiration data for improving hydrological modeling. J. Hydrol. 603, 127046. https://doi.org/10.1016/j.jhydrol.2021.127046.

Shi, S., Zhao, F., Ren, X., Meng, Z., Dang, X., Wu, X., 2022. Soil infiltration properties are affected by typical plant communities in a semi-arid desert grassland in China. Water 14 (20), 3301. https://doi.org/10.3390/w14203301.

Simunek, J., van Genuchten, M.T., 1999. Using the HYDRUS-1D and HYDRUS-2D codes for estimating unsaturated soil hydraulic and solute transport parameters. Charact. Meas. Hydraul. Prop. Unsatur. Porous Media 1. ⟨https://www.ars.usda.gov/arsuserfiles/20360500/pdf_pubs/P1667.pdf⟩, 523-1.

Sirisena, T.J.G., Maskey, S., Ranasinghe, R., 2020. Hydrological model calibration with streamflow and remote sensing-based evapotranspiration data in a data poor basin. Remote Sens. 12 (22), 3768. https://doi.org/10.3390/rs12223768.

Soil Conservation Service-USDA, 1972. Estimation of direct runoff from storm rainfall. National engineering handbook. Sect. 4Hydrol. 10.1–10.24. ⟨https://irrigationtoolbox.com/NEH/Part630_Hydrology/H_210_630_10.pdf⟩.

Souza, V.D.A., Roberti, D.R., Ruhoff, A.L., Zimmer, T., Adamatti, D.S., Gonçalves, L.G.G. D., Moraes, O.L.D., 2019. Evaluation of MOD16 algorithm over irrigated rice paddy using flux tower measurements in Southern Brazil. Water 11 (9), 1911. https://doi.org/10.3390/w11091911.

Srinivasan, R., Zhang, X., Arnold, J., 2010. SWAT ungauged: hydrological budget and crop yield predictions in the upper Mississippi River basin. Trans. ASABE 53 (5), 1533–1546. https://doi.org/10.13031/2013.34903.

Srivastava, A., Kumari, N., Maza, M., 2020. Hydrological response to agricultural land use heterogeneity using variable infiltration capacity model. Water Resour. Manag. 34 (12), 3779–3794. https://doi.org/10.1007/s11269-020-02630-4.

Sugathan, N., Biju, V., Renuka, G., 2014. Influence of soil moisture content on surface albedo and soil thermal parameters at a tropical station. J. Earth Syst. Sci. 123 (5), 1115–1128. https://doi.org/10.1007/s12040-014-0452-x.

Sun, J., Hou, G., Liu, M., Fu, G., Zhan, T., Zhou, H., Haregeweyn, N., 2019. Effects of climatic and grazing changes on desertification of alpine grasslands, Northern Tibet. Ecol. Indic. 107, 105647. https://doi.org/10.1016/j.ecolind.2019.105647.

SWAT+ Gitbook, 2023. SWAT+ Theoretical Documentation. [online] Available at: ⟨https://swatplus.gitbook.io⟩ [Accessed Aug 2025].

Taia, S., Scozzari, A., Erraioui, L., Kili, M., Mridekh, A., Haida, S., El Mansouri, B., 2023. Comparing the ability of different remotely sensed evapotranspiration products in enhancing hydrological model performance and reducing prediction uncertainty. Ecol. Inform. 78, 102352. https://doi.org/10.1016/j.ecoinf.2023.102352.

Tang, R., Shao, K., Li, Z.L., Wu, H., Tang, B.H., Zhou, G., Zhang, L., 2015. Multiscale validation of the 8-day MOD16 evapotranspiration product using flux data collected in China. IEEE J. Sel. Top. Appl. Earth Obs. Remote Sens. 8 (4), 1478–1486. https://doi.org/10.1109/JSTARS.2015.2420105.

Tarantola, S., Gatelli, D., Mara, T.A., 2006. Random balance designs for the estimation of first order global sensitivity indices. Reliab. Eng. Syst. Saf. 91 (6), 717–727. https://doi.org/10.1016/j.ress.2005.06.003.

Tenreiro, T.R., García-Vila, M., Gómez, J.A., Jimenez-Berni, J.A., Fereres, E., 2020. Water modelling approaches and opportunities to simulate spatial water variations at crop field level. Agric. Water Manag. 240, 106254. https://doi.org/10.1016/j.agwat.2020.106254.

Tessema, S.M., 2011. Hydrological modeling as a tool for sustainable water resources management: a case study of the Awash River Basin (Doctoral dissertation, KTH Royal Institute of Technology). ⟨https://urn.kb.se/resolve?urn=urn%3Anbn%3Ase%3Akth%3Adiva-33617⟩.

Tobin, K.J., Bennett, M.E., 2017. Constraining SWAT calibration with remotely sensed evapotranspiration data. JAWRA J. Am. Water Resour. Assoc. 53, 593–604. https://doi.org/10.1111/1752-1688.12516.

Tognetti, R., d'Andria, R., Lavini, A., Morelli, G., 2006. The effect of deficit irrigation on crop yield and vegetative development of olea europaea L. (cultivars Frantoio and Leccino). Eur. J. Agron. 25 (4), 356–364. https://doi.org/10.1016/j.eja.2006.07.003.

Tolson, B.A., Shoemaker, C.A., 2007. Cannonsville reservoir watershed SWAT2000 model development, calibration and validation. J. Hydrol. 337 (1–2), 68–86. https://doi.org/10.1016/j.jhydrol.2007.01.017.

Tramblay, Y., Koutroulis, A., Samaniego, L., Vicente-Serrano, S.M., Volaire, F., Boone, A., Polcher, J., 2020. Challenges for drought assessment in the Mediterranean region under future climate scenarios. EarthSci. Rev. 210, 103348. https://doi.org/10.1016/j.earscirev.2020.103348.

Villani, L., Castelli, G., Yimer, E.A., Chawanda, C.J., Nkwasa, A., Van Schaeybroeck, B., Penna, D., van Griensven, A., Bresci, E., 2024a. Impacts of climate change and vegetation response on future aridity in a Mediterranean catchment. Agric. Water Manag. 299, 108878. https://doi.org/10.1016/j.agwat.2024.108878.

Villani, L., Castelli, G., Yimer, E.A., Nkwasa, A., Penna, D., van Griensven, A., Bresci, E., 2024b. Exploring adaptive capacities in Mediterranean agriculture: insights from central Italy's ombrone catchment. Agric. Syst. 216, 103903. https://doi.org/10.1016/j.agsy.2024.103903.

Visakh, S., Raju, P.V., Kulkarni, S.S., Diwakar, P.G., 2019. Inter-comparison of water balance components of river basins draining into selected delta districts of eastern India. Sci. Total Environ. 654, 1258–1269. https://doi.org/10.1016/j.scitotenv.2018.11.162.

Wagner, P.D., Bieger, K., Arnold, J.G., Fohrer, N., 2022. Representation of hydrological processes in a rural lowland catchment in Northern Germany using SWAT and SWAT +. Hydrol. Process. 36 (5), e14589. https://doi.org/10.1002/hyp.14589.

Wahren, F.T., Julich, S., Nunes, J.P., Gonzalez-Pelayo, O., Hawtree, D., Feger, K.H., Keizer, J.J., 2016. Combining digital soil mapping and hydrological modeling in a data scarce watershed in north-central Portugal. Geoderma 264, 350–362. https://doi.org/10.1016/j.geoderma.2015.08.023.

Weerasinghe, I., Bastiaanssen, W., Mul, M., Jia, L., Van Griensven, A., 2020. Can we trust remote sensing evapotranspiration products over Africa? Hydrol. Earth Syst. Sci. 24, 1565–1586. https://doi.org/10.5194/hess-24-1565-2020.

Williams, J.R., 1995. The EPIC model. In: Singh, V.P. (Ed.), Computer Models of Watershed Hydrology. Water Resources Publications, Highlands Ranch, Colorado, pp. 909–1000.

Winsemius, H.C., Savenije, H.H.G., Bastiaanssen, W.G.M., 2008. Constraining model parameters on remotely sensed evaporation: justification for distribution in ungauged basins? Hydrol. Earth Syst. Sci. Discuss. 5, 2293–2318. https://doi.org/10.5194/hessd-5-2293-2008.

Wu, K., Johnston, C.A., 2007. Hydrologic response to climatic variability in a great lakes watershed: a case study with the SWAT model. J. Hydrol. 337 (1-2), 187–199. https://doi.org/10.1016/j.jhydrol.2007.01.030.

Xu, T., Guo, Z., Xia, Y., Ferreira, V.G., Liu, S., Wang, K., Zhao, C., 2019. Evaluation of twelve evapotranspiration products from machine learning, remote sensing and land surface models over conterminous United States. J. Hydrol. 578, 124105. https://doi.org/10.1016/j.jhydrol.2019.124105.

Yates, D., Purkey, D., Sieber, J., Huber-Lee, A., Galbraith, H., West, J., Herrod-Julius, S., 2007. A physically-based, water resource planning model of the Sacramento basin, california USA. ASCE J. Water Resour. Plan. Manag. 1–32. https://doi.org/10.1016/j.ejrh.2024.101846.

Yen, H., Park, S., Arnold, J.G., Srinivasan, R., Chawanda, C.J., Wang, R., Zhang, X., 2019. IPEAT+: a built-in optimization and automatic calibration tool of SWAT+. Water 11 (8), 1681. https://doi.org/10.3390/w11081681.

Yulianti, M., Özkundakci, D., Ridwansyah, I., 2025. Simulating water balance and nutrient losses in a pastoral catchment using the SWAT+ model: added value of isotope data. Hydrol. Sci. J. 70 (1), 127–143. https://doi.org/10.1080/02626667.2024.2423047.